Novel Light Dark Matter Detection with Quantum Parity Detector Using Qubit Arrays

Ningqiang Song

with Xuegang Li, Yuxiang Liu, Jing Shu, Yidong Song, Junhua Wang, Yue-Liang Wu, Tiantian Zhang, and Yu-Feng Zhou

Institute of Theoretical Physics, Chinese Academy of Sciences

July 16th, 2026

Evidence of Dark Matter in our Universe

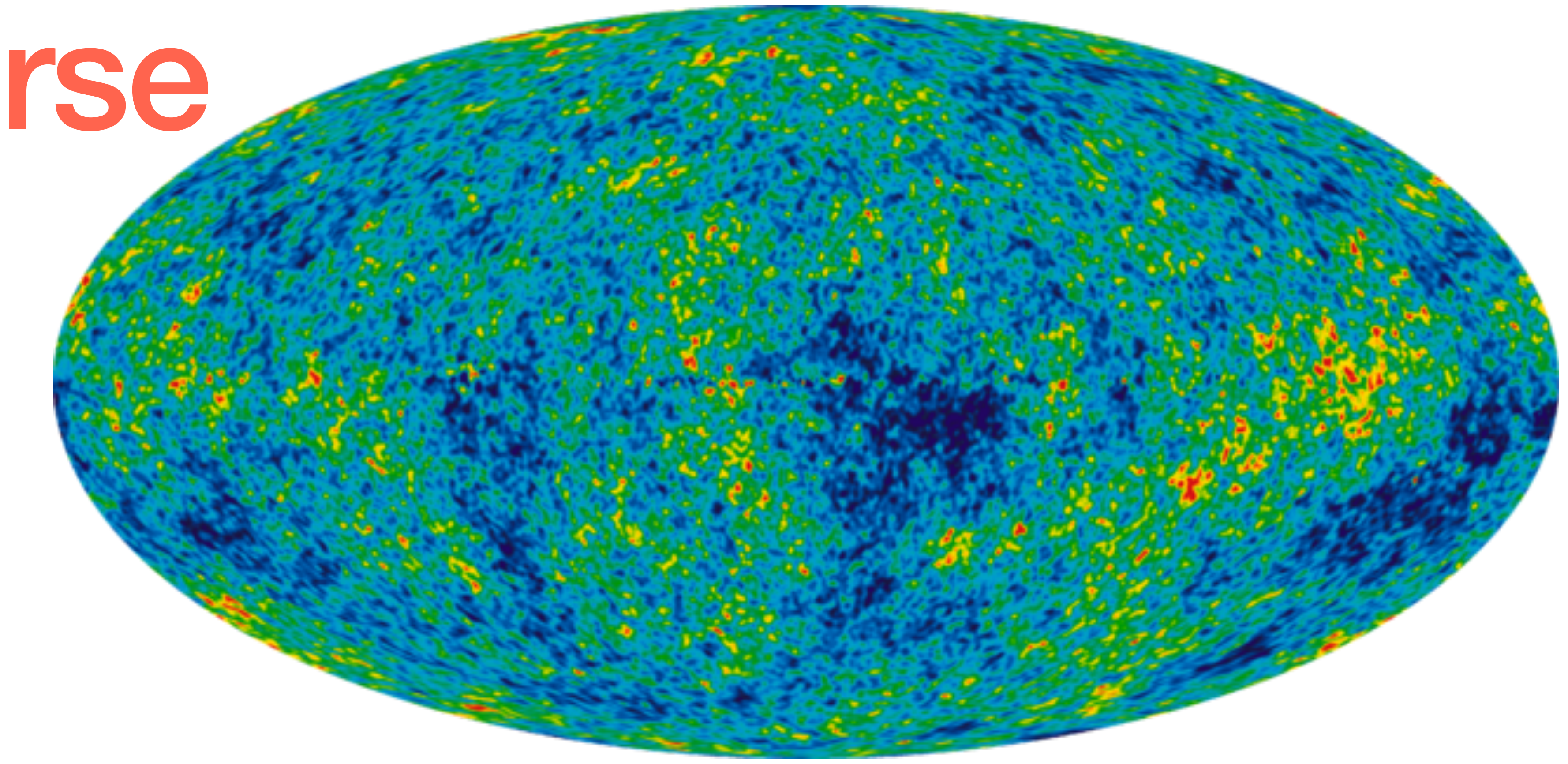

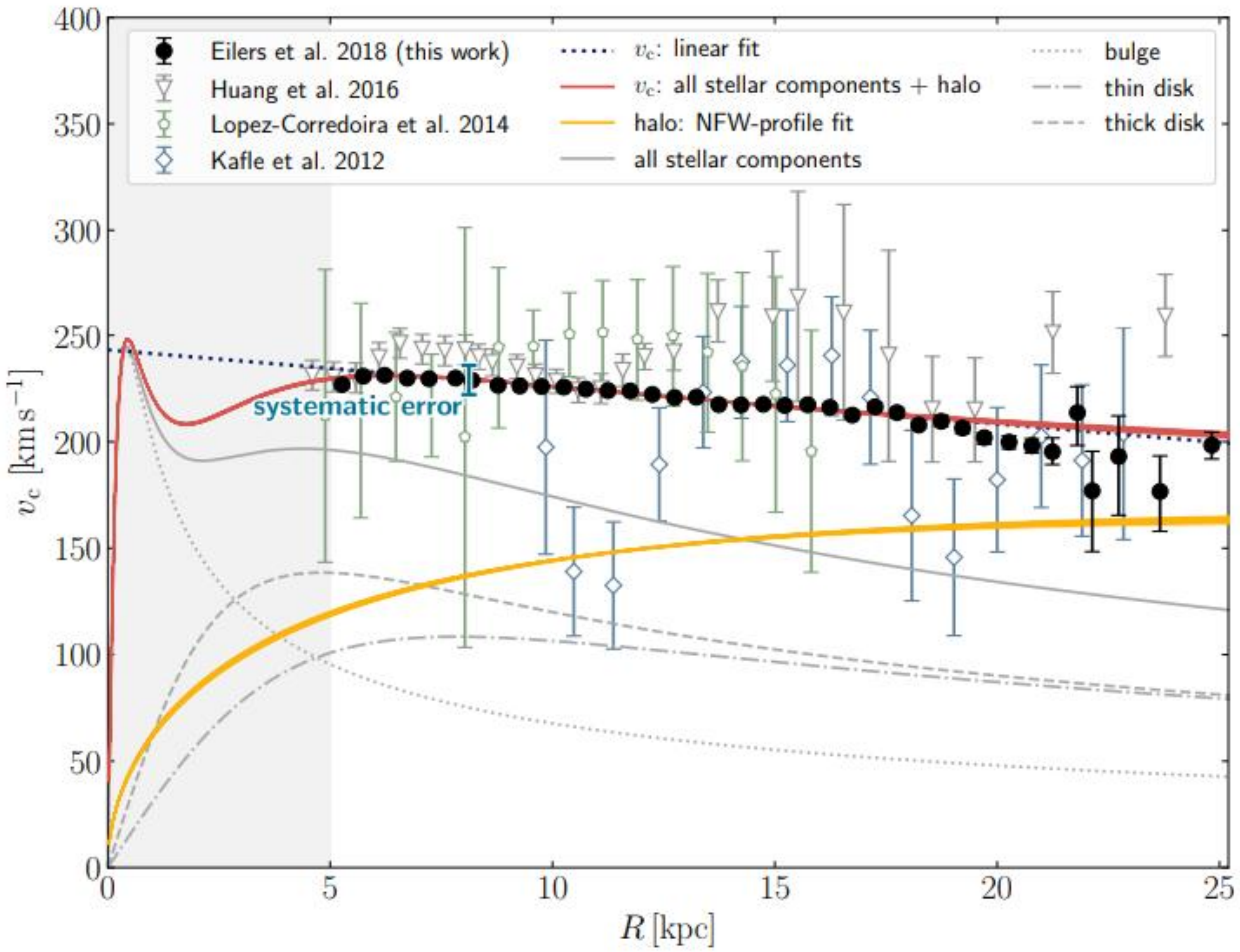

Eilers *et al.*, 1810.09466

The Dark Matter Candidates

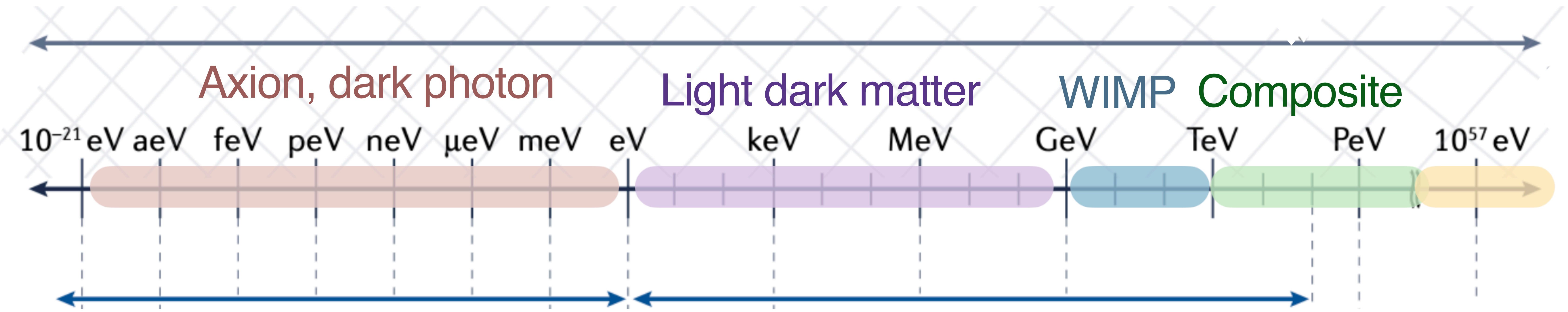

Dark matter mass

Wave-like dark matter

Particle-like dark matter

Black hole

Nature Viewpoint, 4, 637-641

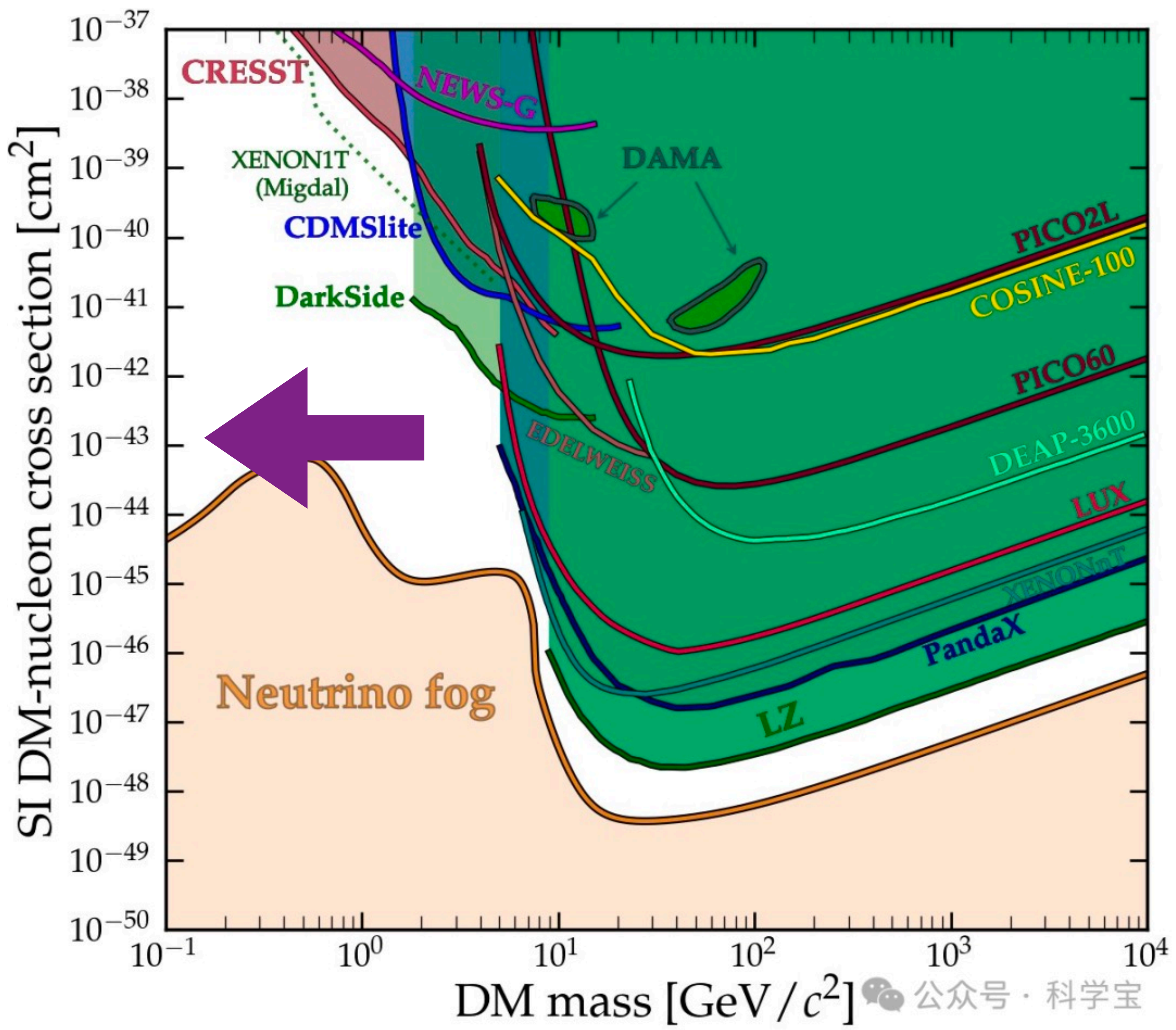

LZ 2207.03764

XENONnT 2303.14729

PandaX-4t 2408.00664

LZ 2410.17036

Dark matter might be lighter than we thought

Kinematics of Light Dark Matter

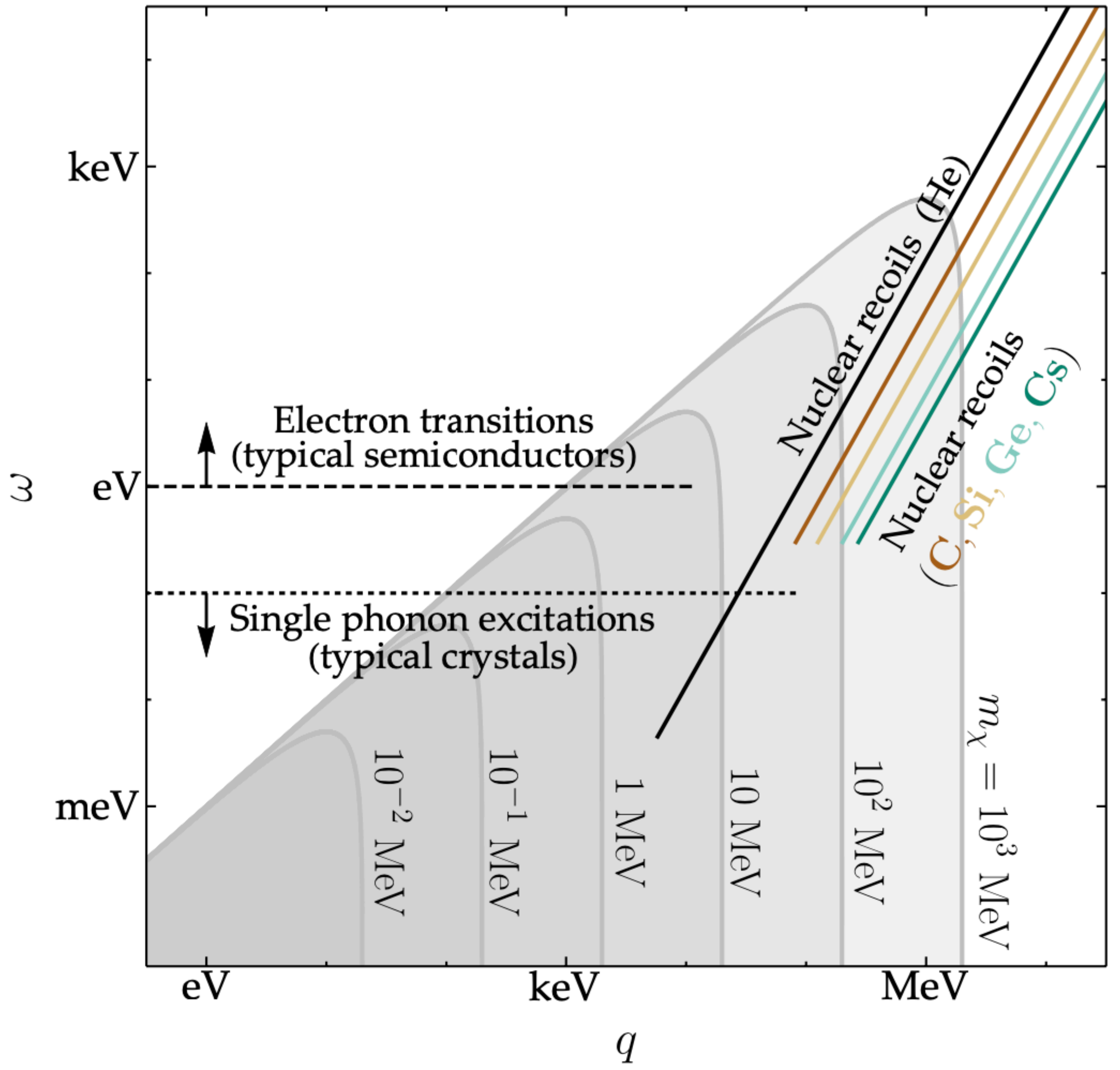

1910.08092

- The maximum dark matter energy deposition depends on its mass
- The energy deposition reduces for lower mass dark matter

$$\omega_{\boldsymbol{q}} = \frac{1}{2} m_\chi v^2 - \frac{(m_\chi \boldsymbol{v} - \boldsymbol{q})^2}{2m_\chi} = \boldsymbol{q} \cdot \boldsymbol{v} - \frac{q^2}{2m_\chi}$$

$$E_{\text{dep}} \leq E_k \sim m_{\text{DM}} v^2 \sim 10^{-6} m_{\text{DM}}$$

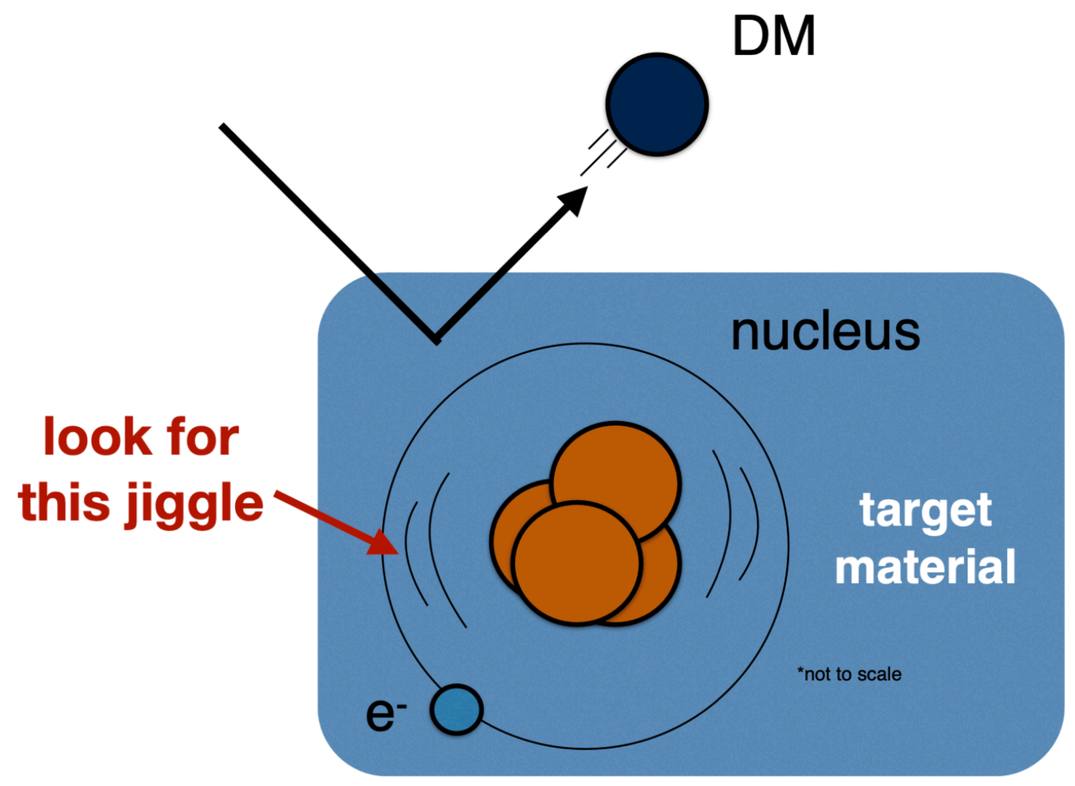

Tientien Yu, IAS-HEP 2023

Superconducting Qubits as Dark Matter Detector

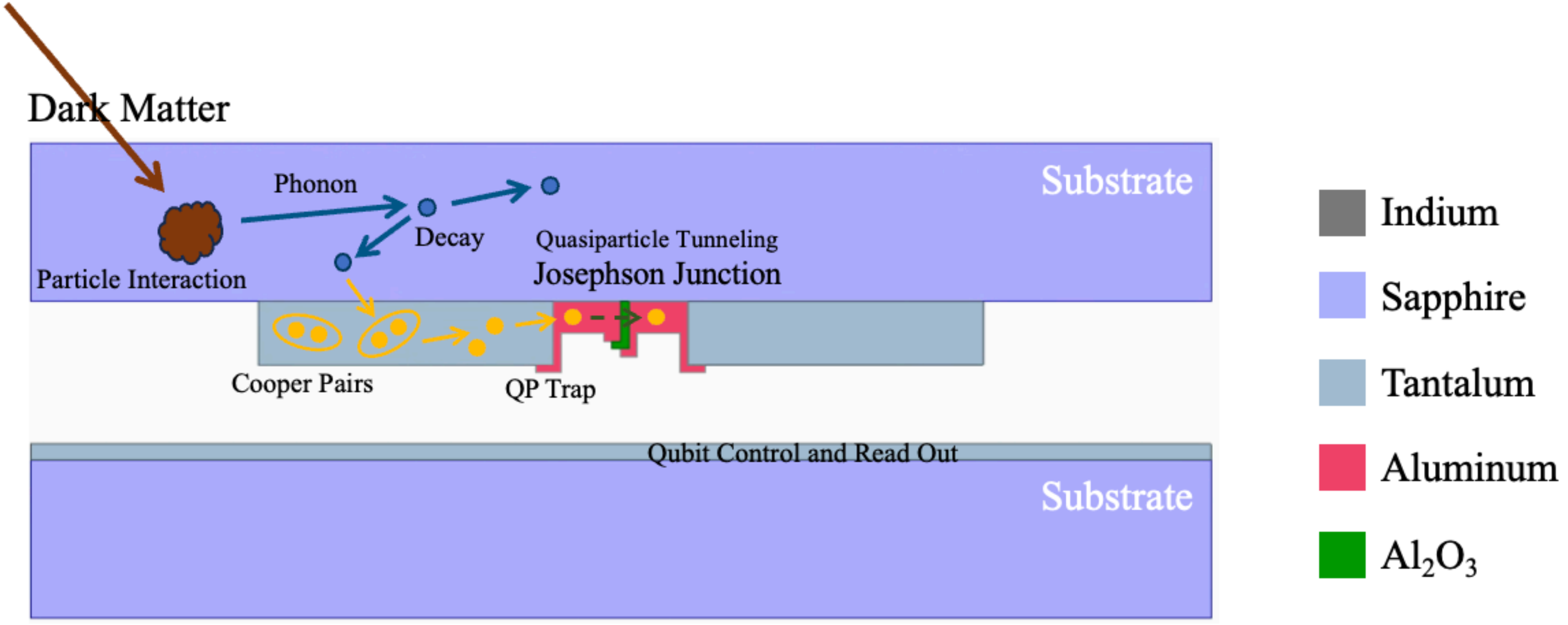

- **Dark matter scatters and produces phonons in the substrate, which generates quasiparticles in the island**
- **The tunnelling of quasiparticles yields detectable signals**
- **Trapping setup to concentrate quasiparticles**

The Experimental Setup

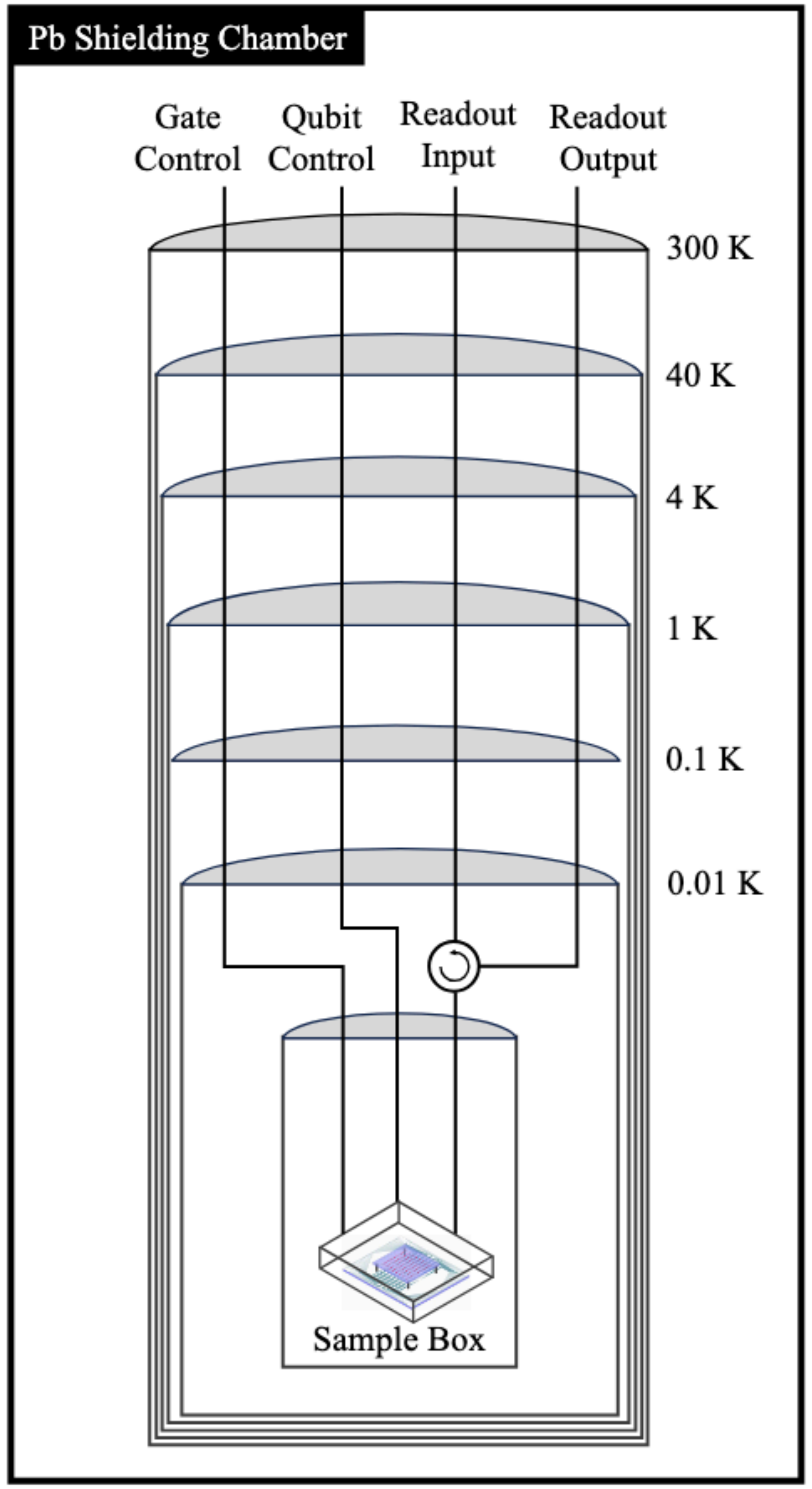

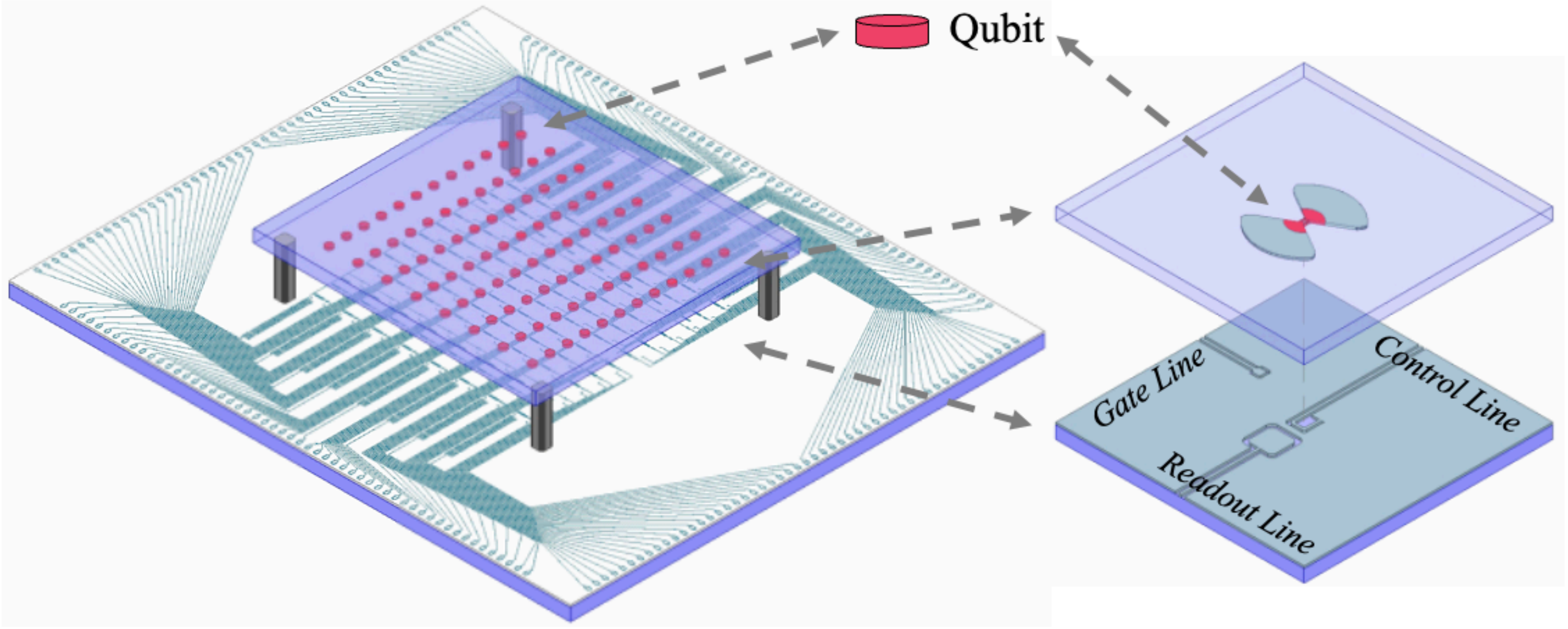

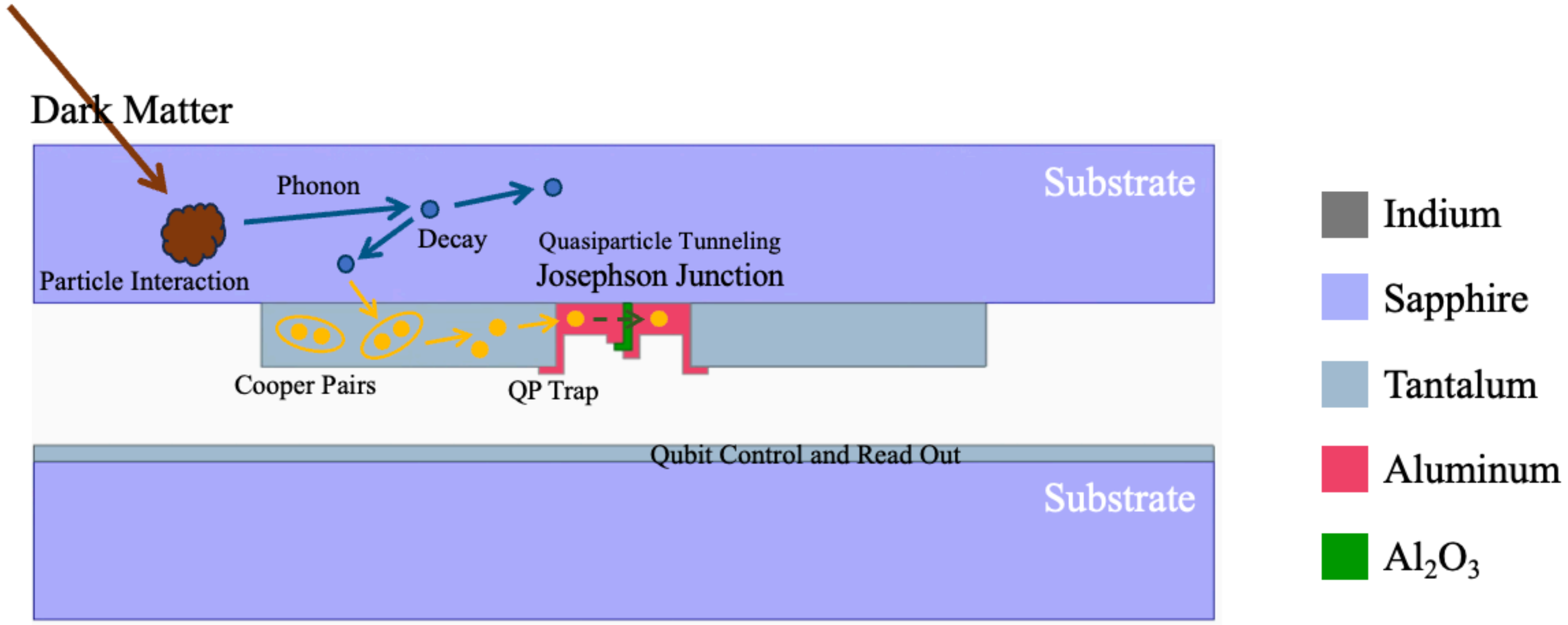

Dark Matter Scattering Rate

PhonoDark: https://github.com/tanner-trickle/PhonoDark

See also: 1910.08092, 2009.13534

$$\Gamma(\boldsymbol{v}) = V \int \frac{d^3q}{(2\pi)^3} \sum_f \left| \langle \boldsymbol{p}', f | \, \delta \hat{H} \, | \boldsymbol{p}, i \rangle \right|^2 2\pi \delta\left(E_f - E_i - \omega_{\boldsymbol{q}}\right)$$

$$R = \frac{1}{\rho_T} \frac{\rho_\chi}{m_\chi} \int d^3v \, f_\chi(\boldsymbol{v}) \, \Gamma(\boldsymbol{v})$$

$$R = \frac{1}{m_{\text{cell}}} \frac{\rho_\chi}{m_\chi} \frac{\pi \bar{\sigma}}{2\mu^2} \int \frac{d^3q}{(2\pi)^3} \mathcal{F}^2_{\text{med}}(q) \sum_\nu \frac{1}{\omega_{\nu,\boldsymbol{k}}} \left| \sum_j \frac{e^{-W_j(\boldsymbol{q})}}{\sqrt{m_j}} e^{i\boldsymbol{G}\cdot\boldsymbol{x}_j^0} \left(\boldsymbol{Y}_j \cdot \boldsymbol{\epsilon}^*_{\nu,\boldsymbol{k},j}\right) \right|^2 g(\boldsymbol{q}, \omega_{\nu,\boldsymbol{k}})$$

Cell mass

Mediator form factor

Phonon eigen energy

Material response

Dark matter velocity integral

Sapphire

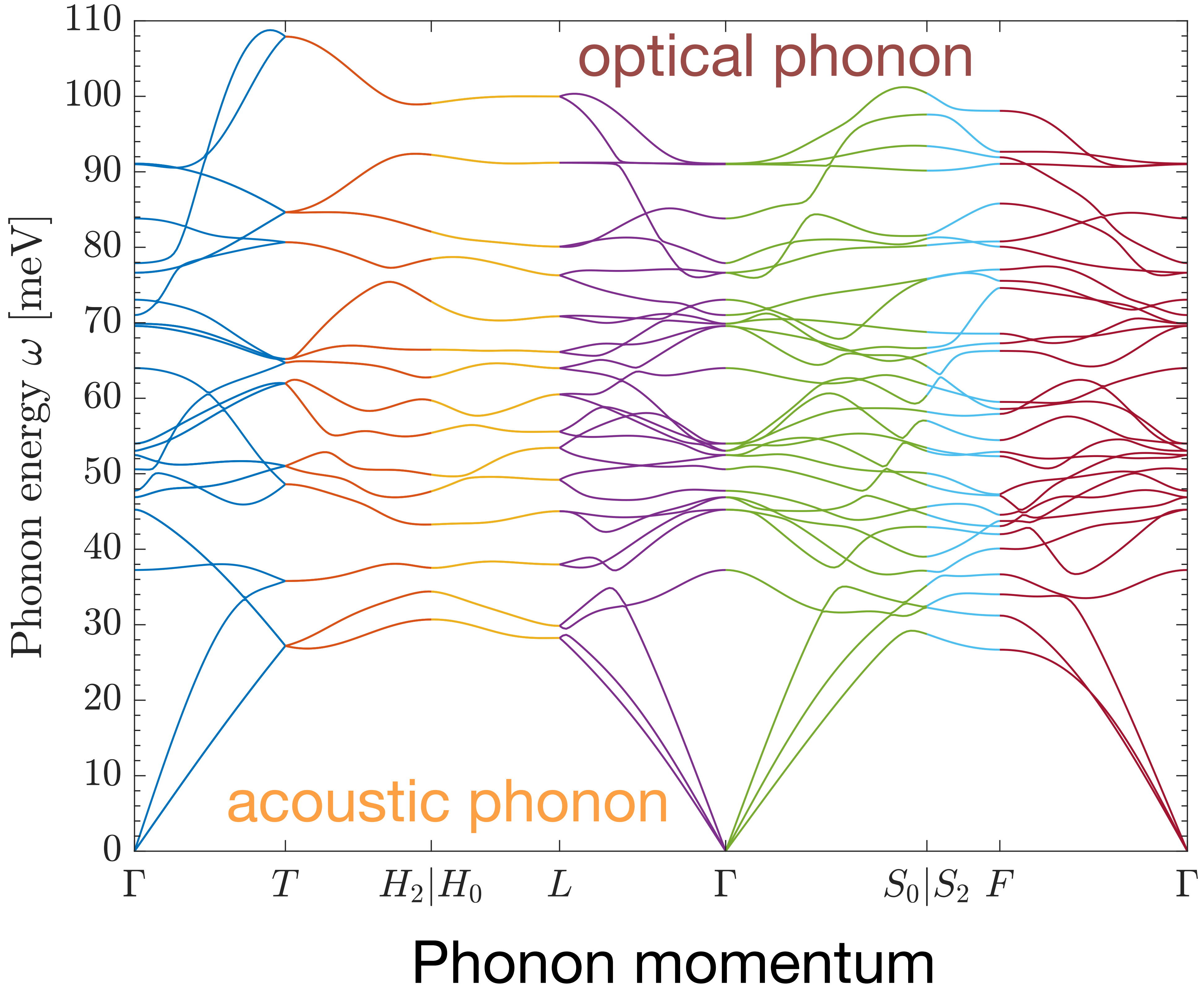

Phonon Simulations

G4CMP

- Anharmonic down-conversion of longitudinal phonon
- Isotopic scattering of transverse phonon

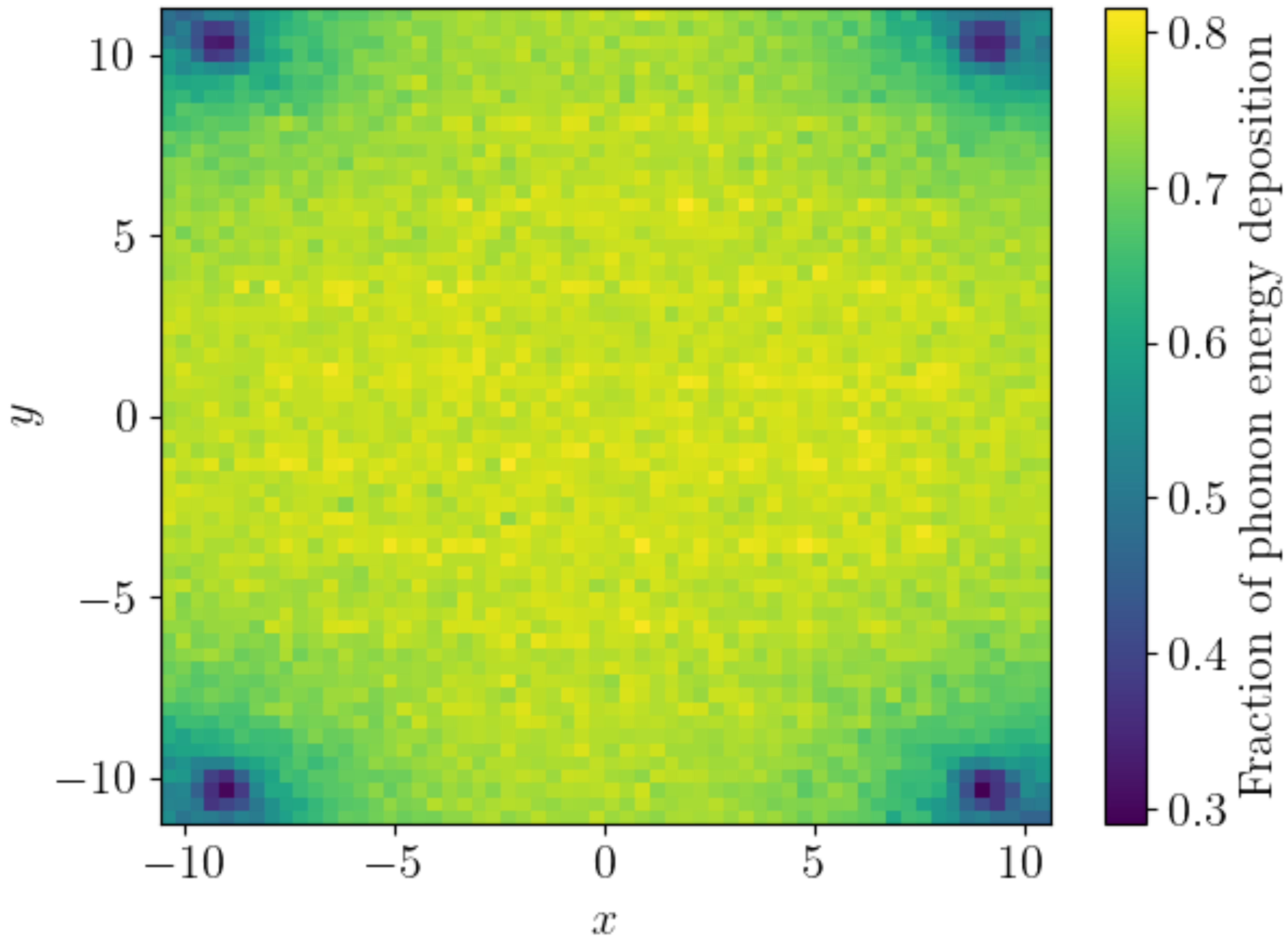

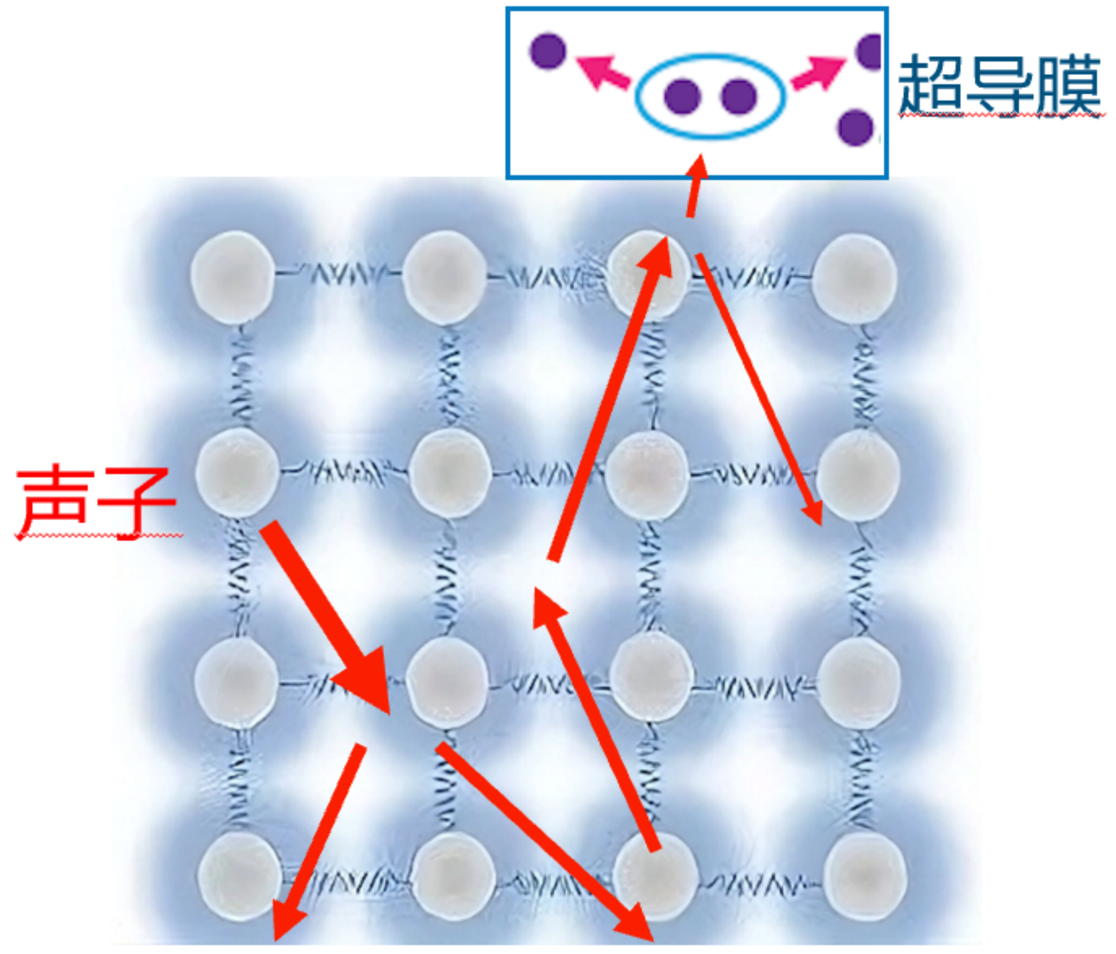

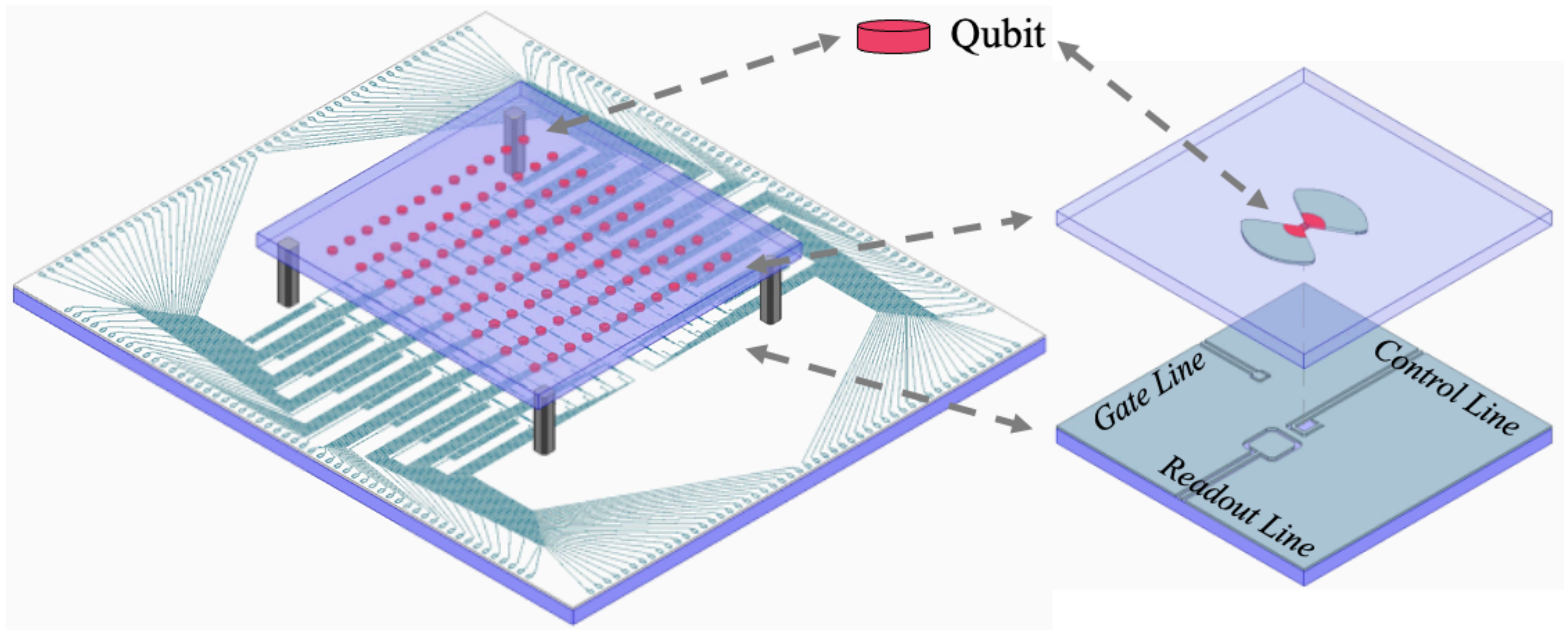

- **96 qubits to enhance phonon collection efficiency**
- **Separate the Qubit chip from the Carrier chip to minimize energy dissipation**

Quantum Parity Measurements

charge parity $P = \pm 1$

$$H = 4E_C \left(n - n_g + \frac{P - 1}{4}\right)^2 - E_J \cos\phi$$

Charge-parity jumps

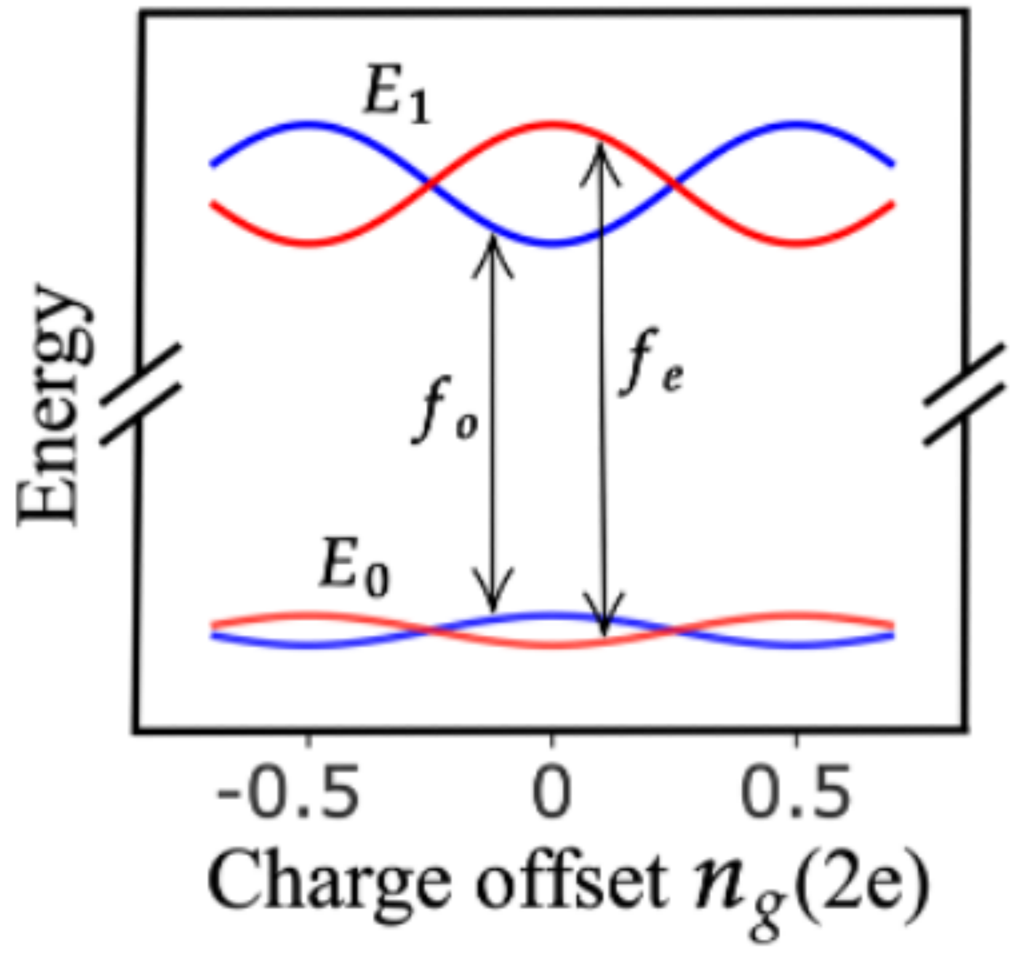

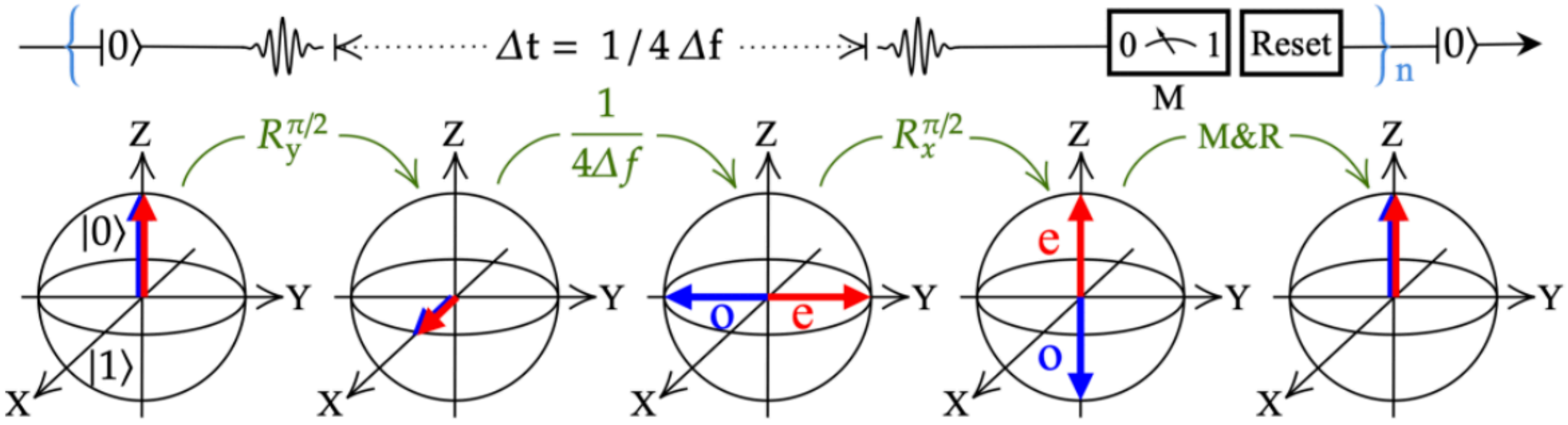

- **The charge-parity state switches between even and odd with slightly different energies when a quasiparticle tunnels in the Josephson junction**
- **Mapping the charge-parity state onto |0> or |1> with distinct transition frequencies, which accumulate over time to a phase difference of π in the readout**
- **Sensitive to single quasiparticle tunneling with high time resolution**

Background

- Cosmic ray and radio active decay ⇒ $\omega \gtrsim \text{keV}$
- Soft scattering of high energy gamma
- Residual quasiparticle ⇒ taken into consideration
- Infrared leakage ⇒ isolation and filtering
- Thermal stress ⇒ exponential decay in 6-10 days, wait!

2112.09702

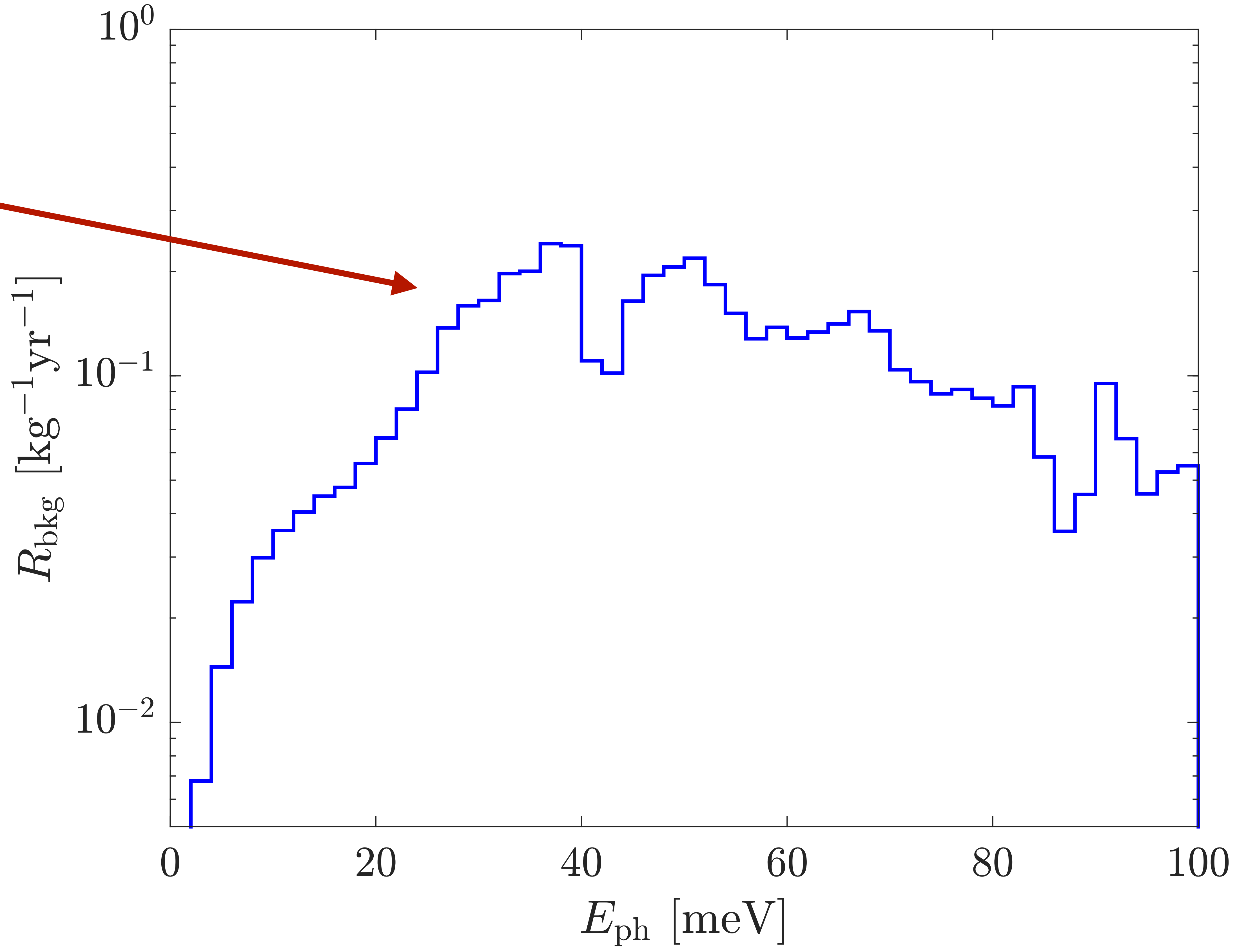

Sensitivity to Light Dark Matter

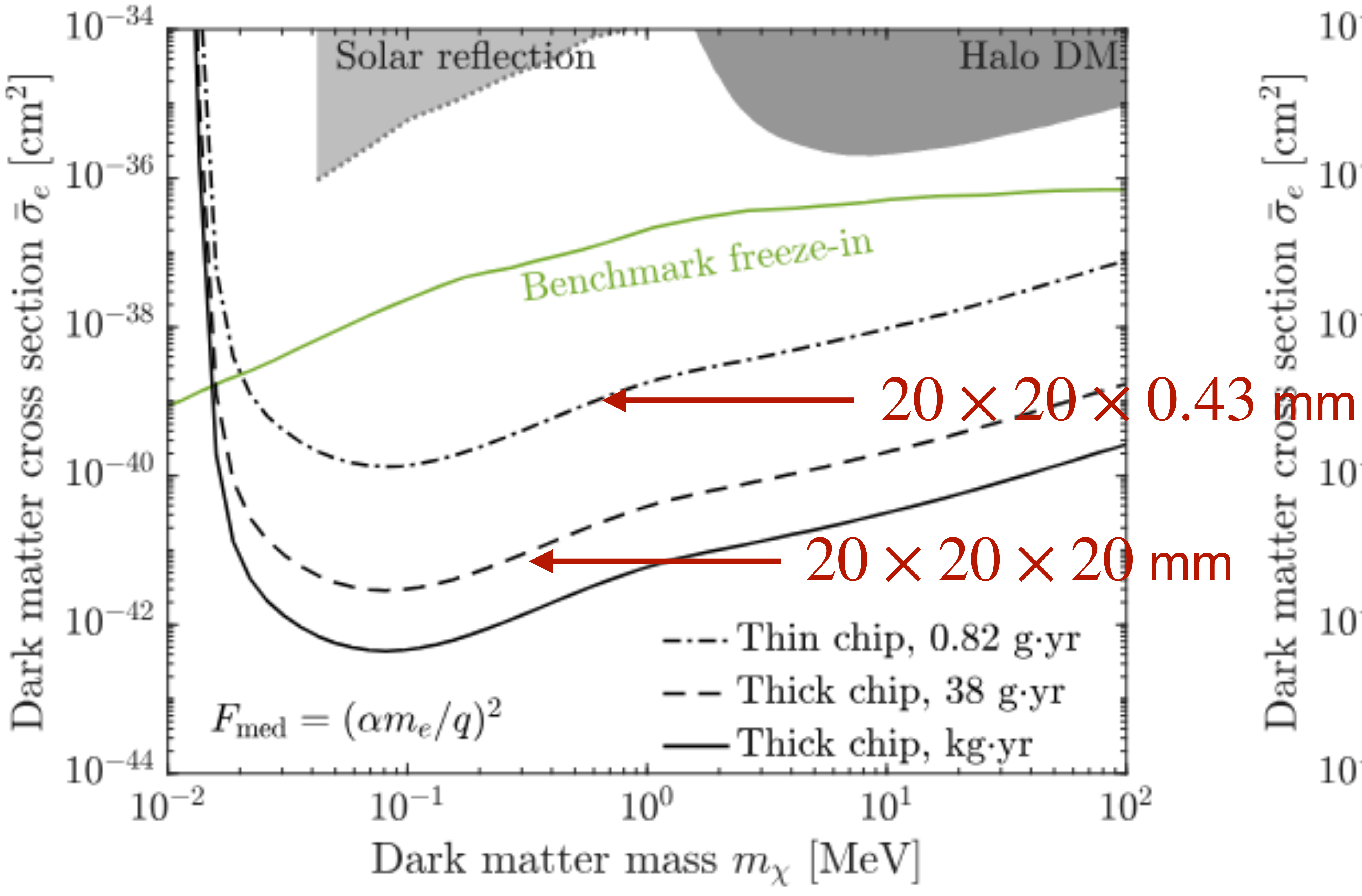

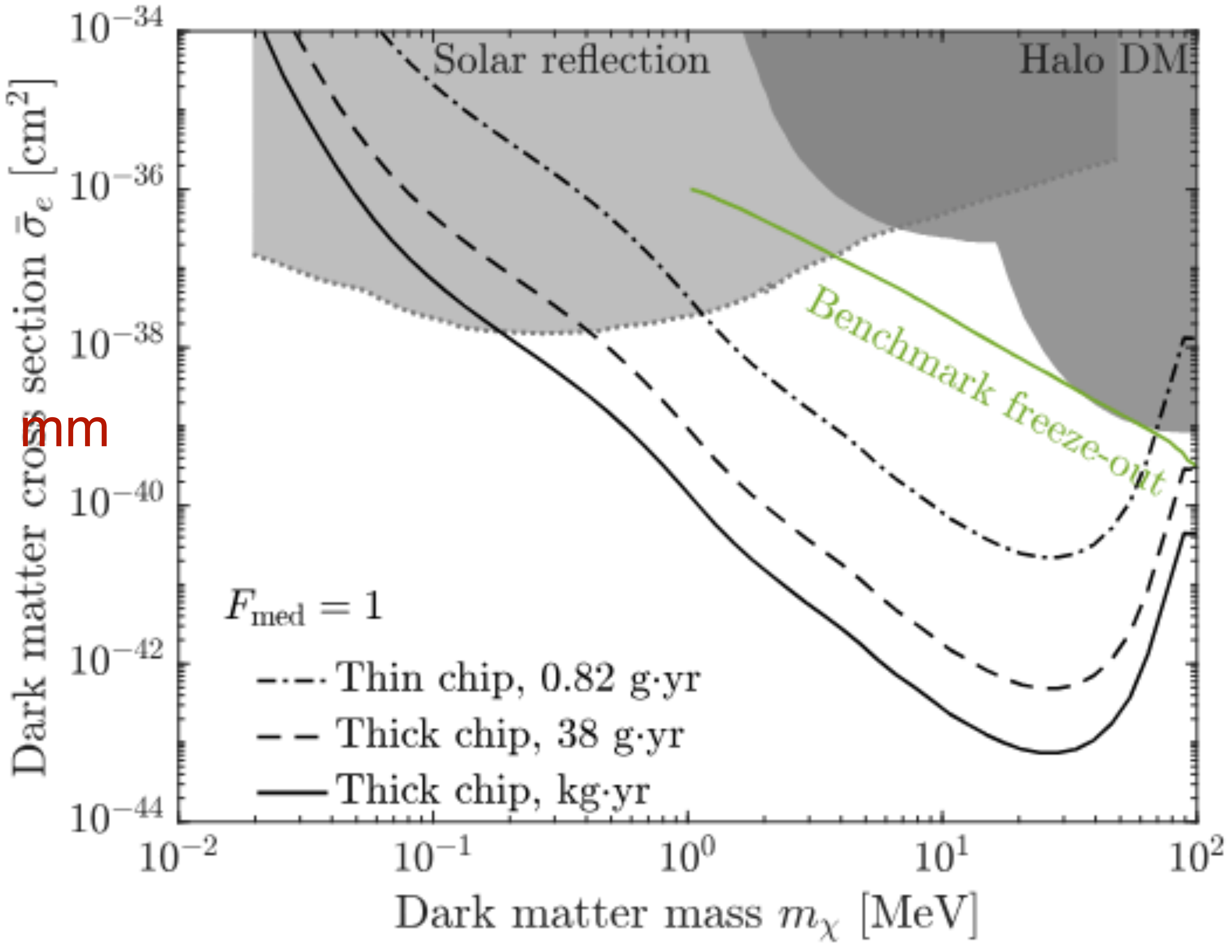

Light mediator **Heavy mediator**

"Novel Light Dark Matter Detection with Quantum Parity Detector Using Qubit Arrays", X. Li, Y. Liu, J. Shu, ***Ningqiang Song***, Y. Song, J. Wang, Y. Wu, T. Zhang, Y. Zhou arXiv: 2512.20309

Sensitivity to Dark Photon and Axion

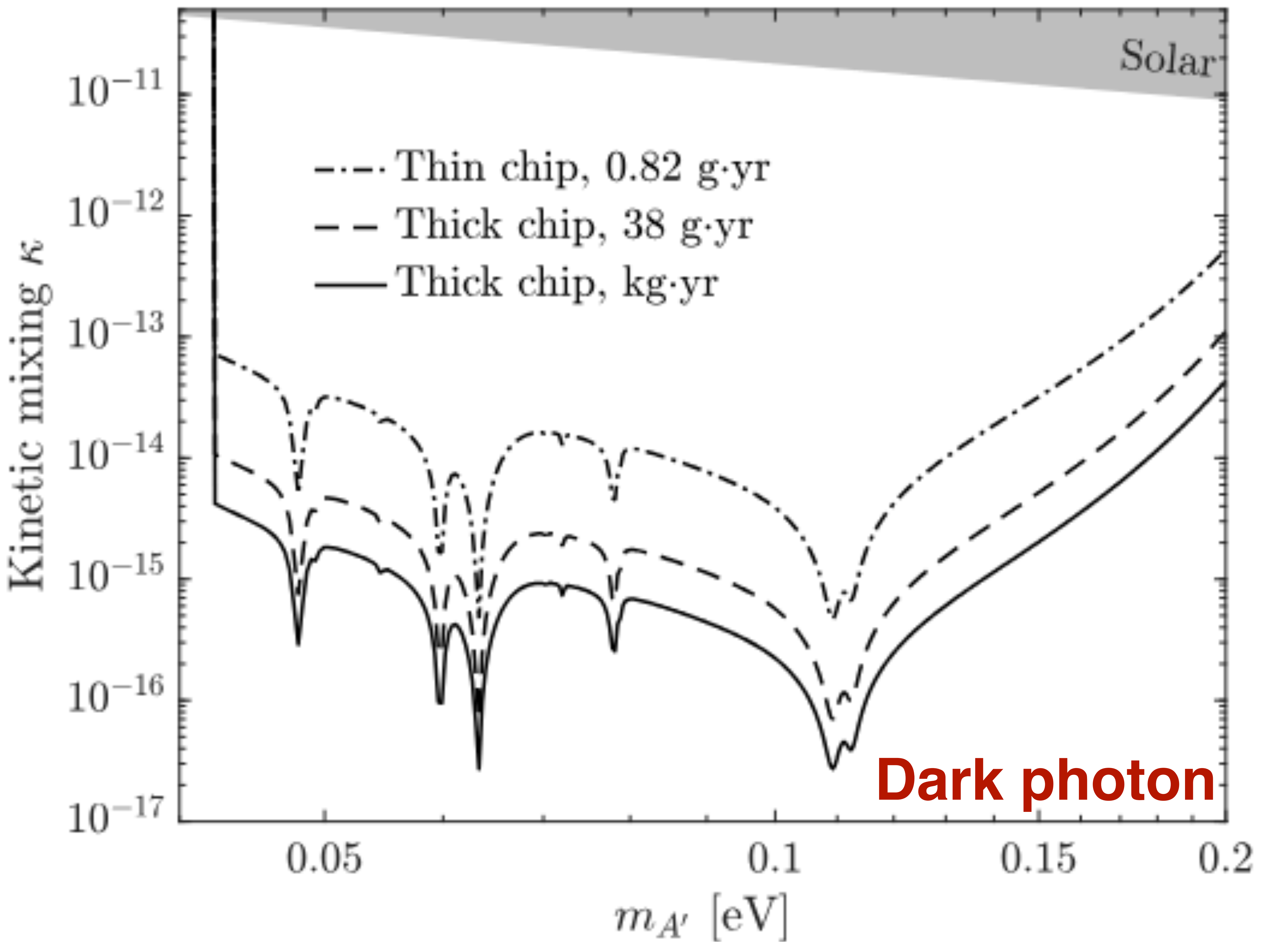

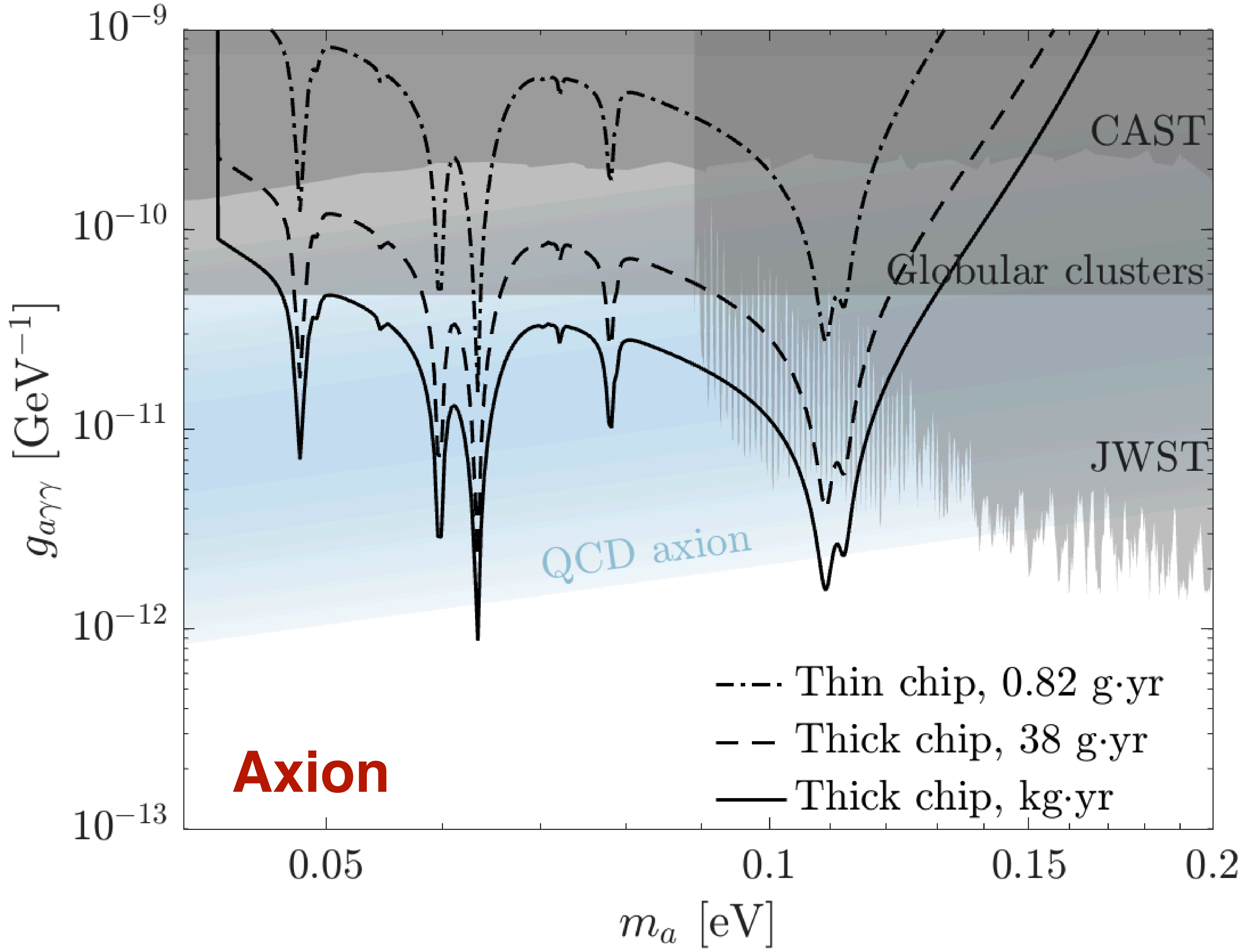

$$R = \frac{1}{\rho_T} \frac{\rho_{A'}}{m_{A'}} \kappa^2 m_{A'} \mathrm{Im}\left[\frac{-1}{\epsilon(m_{A'})}\right]$$

$$R \simeq \left(\frac{g_{a\gamma\gamma} B_0}{m_a}\right)^2 \frac{\rho_{\mathrm{DM}}}{\rho_{\mathrm{T}}} \mathrm{Im}\left[\frac{-1}{\varepsilon(m_a)}\right]$$

"Novel Light Dark Matter Detection with Quantum Parity Detector Using Qubit Arrays", X. Li, Y. Liu, J. Shu, ***Ningqiang Song***, Y. Song, J. Wang, Y. Wu, T. Zhang, Y. Zhou arXiv: 2512.20309

Experimental Status

- Located in the A2 Hall of China JinPing Underground Laboratory (CJPL)
- Qubit chip designed and fabricated
- Qubit chip and calibration light source installed
- First data expected in 2026

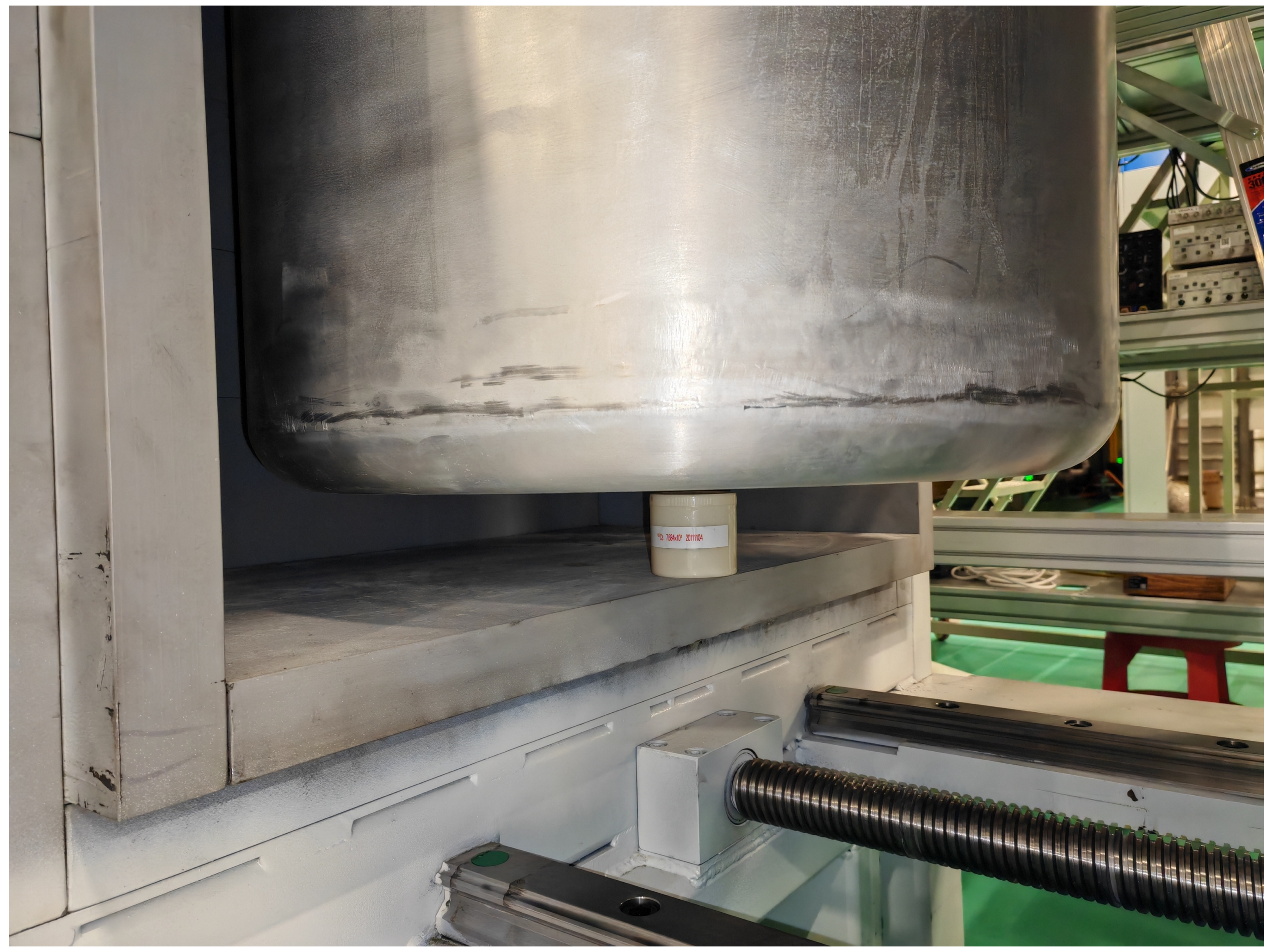

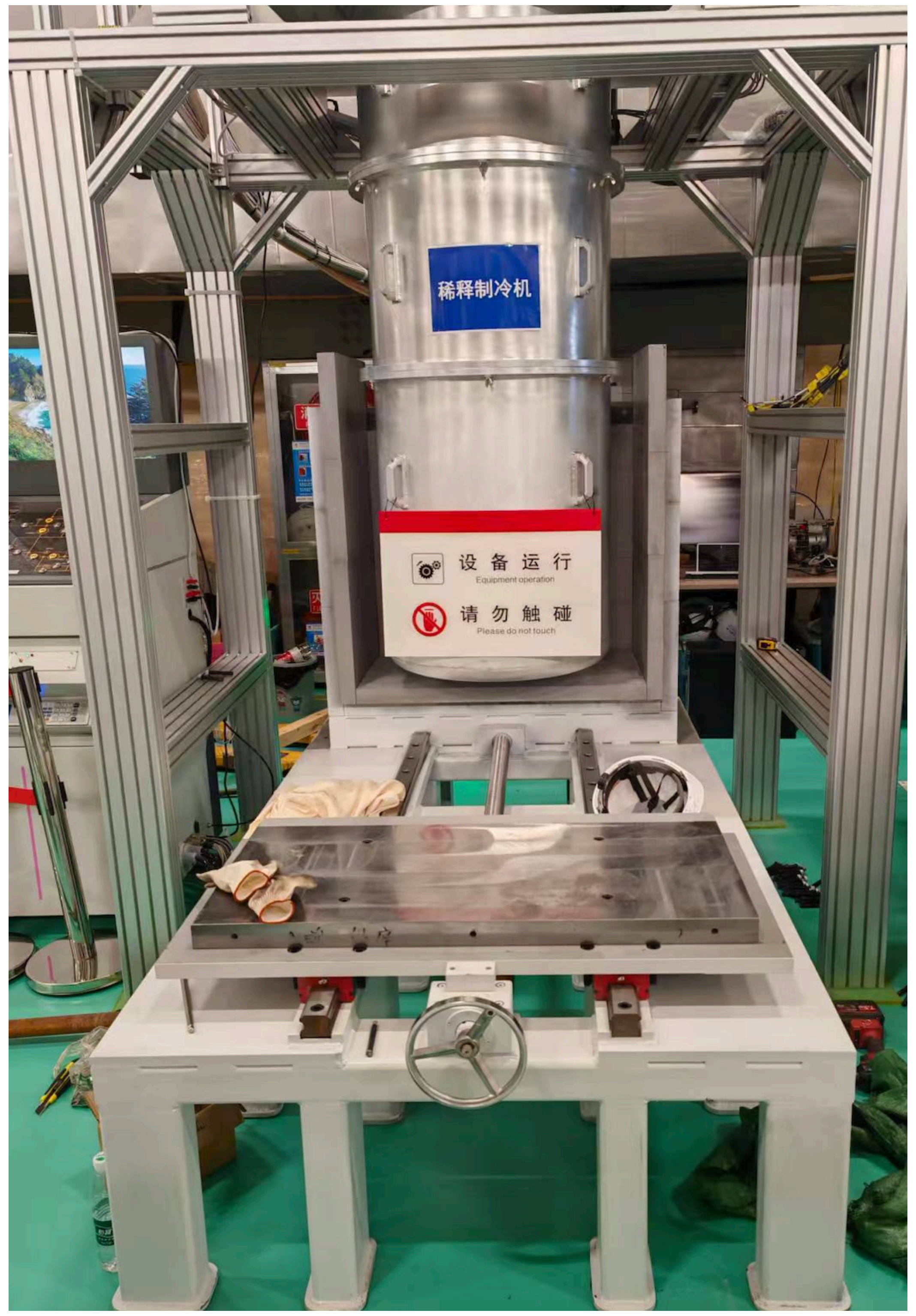

第十五届新物理研讨会

2026·8·23-29 威海金海湾

https://indico.itp.ac.cn/event/420/overview

探索超出粒子物理标准模型的新物理现象和理论规律是当前粒子物理的前沿研究方向，同时与暗物质、暗能量及早期宇宙中的许多重要问题联系紧密。中国科学院理论物理研究所定于2026年8月23日-8月29日（23日报到，29日离会），在威海与山东大学共同举办第十五届“新物理研讨会”，诚邀您参会！

近年来，随着DESI对宇宙大尺度结构的高精度测量以及JWST对高红移星系和早期宇宙结构的深度观测，我们得以以前所未有的精度研究宇宙结构的形成与演化。这些观测为检验暗物质性质以及探索超出标准模型的新物理提供了新的契机和重要线索。 本年度研讨会将以主题综述与专题报告结合的方式举行（上午以邀请综述报告为主，下午以讨论为主），主题集中于宇宙结构形成与暗物质和新物理的内在联系，主要包括宇宙小尺度结构形成、自相互作用暗物质、超轻暗物质、宇宙大尺度结构与暗能量、宇宙早期动力学与随机引力波等。欢迎您参加综述讨论，并在会议上报告相关领域的最新研究成果。

Summary

- Light dark matter typically deposits energy below the experimental threshold
- Design qubit chip to maximum phonon energy deposition and quasiparticle number density
- Dedicated simulations to find the detector threshold and energy resolution
- Expect orders of improvement in the sensitivity for light dark matter
- Experiment undergoing in Beijing and CJPL

Thanks

Back up

SuperCDMS

PRD 104,032010 2021

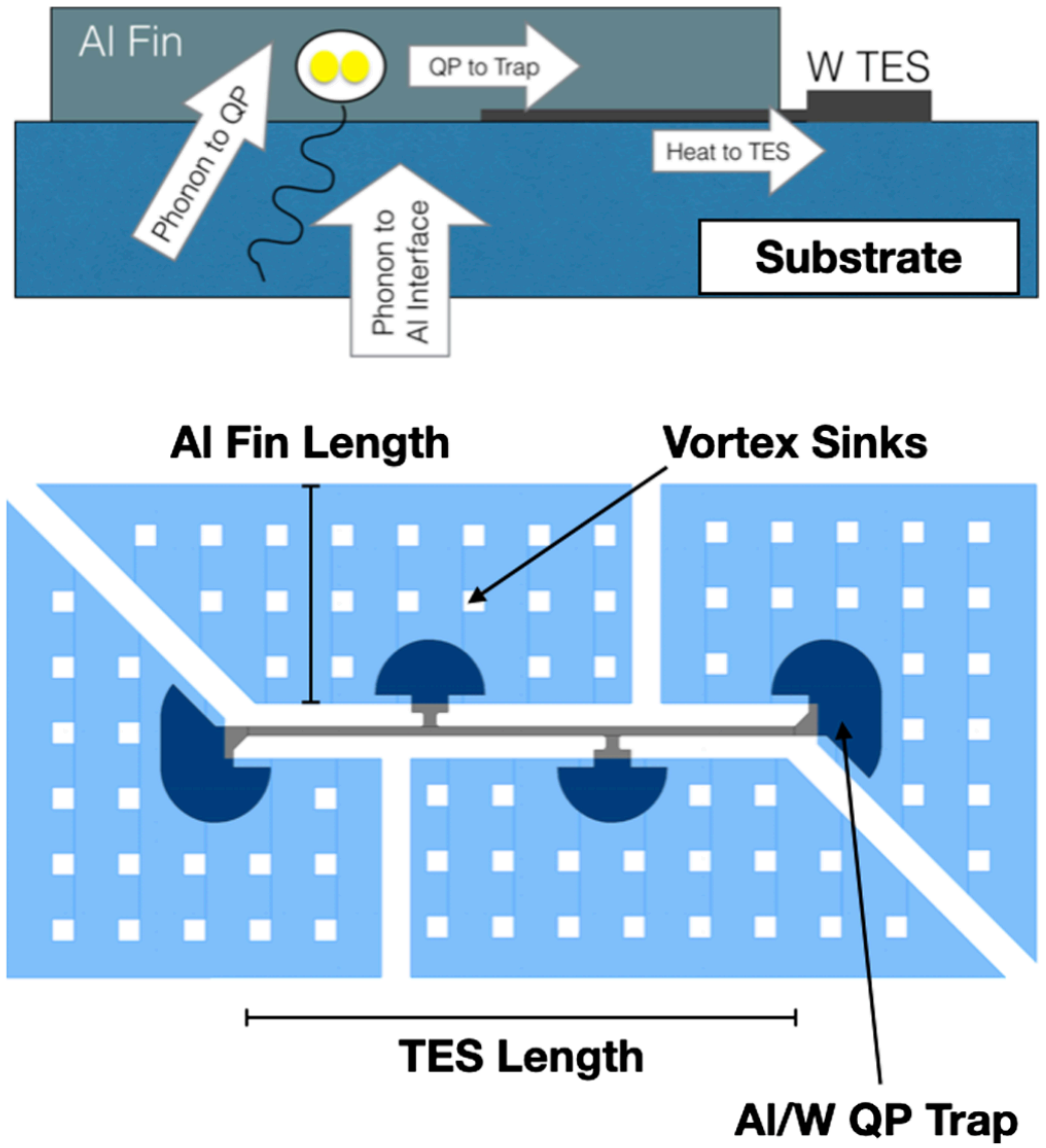

SuperCDMS-CPD phonon+charge

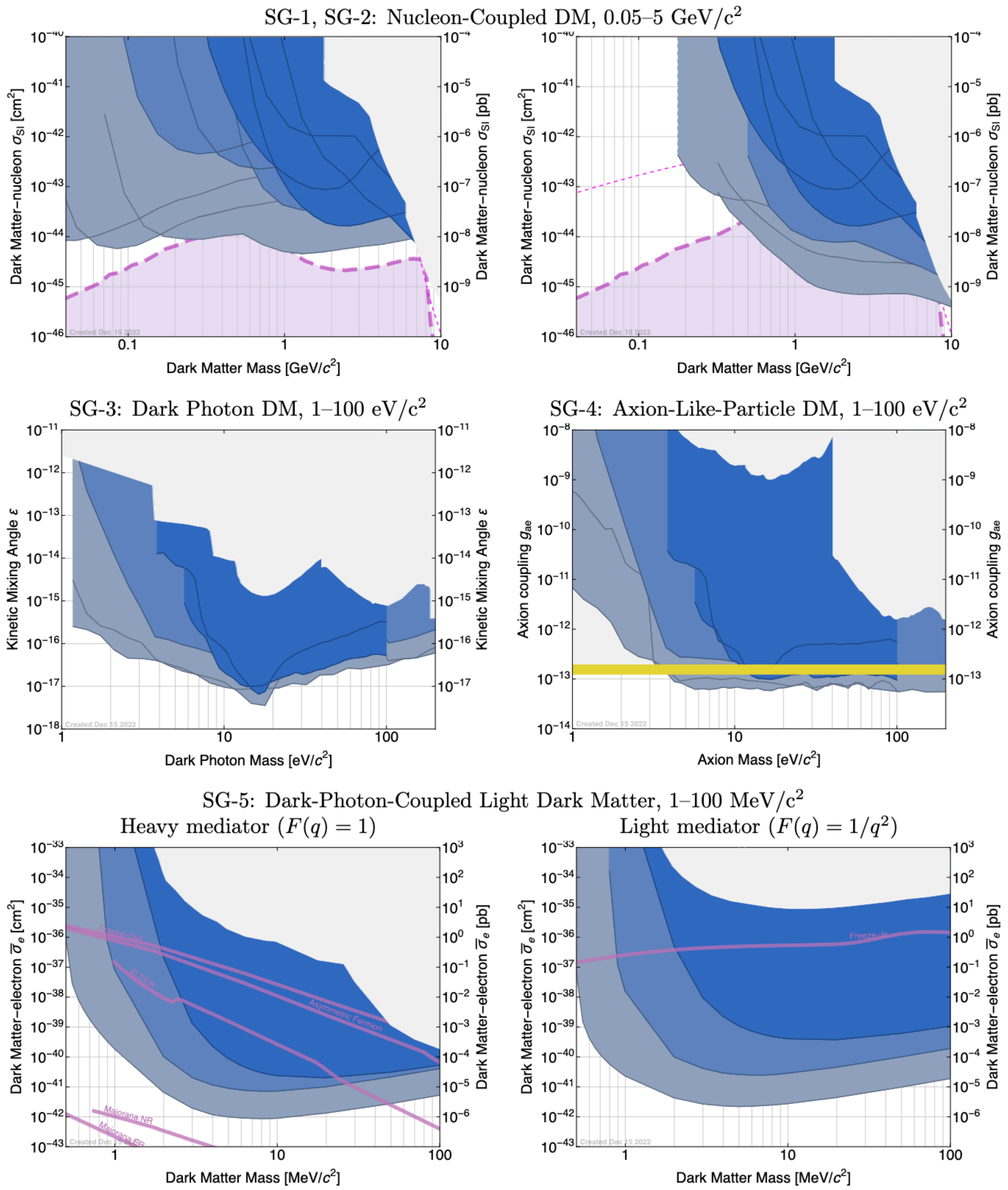

SuperCDMS@SNOLab

$E_{\text{th}} \sim \text{eV}$ 2203.08463

SENSEI/CDEX

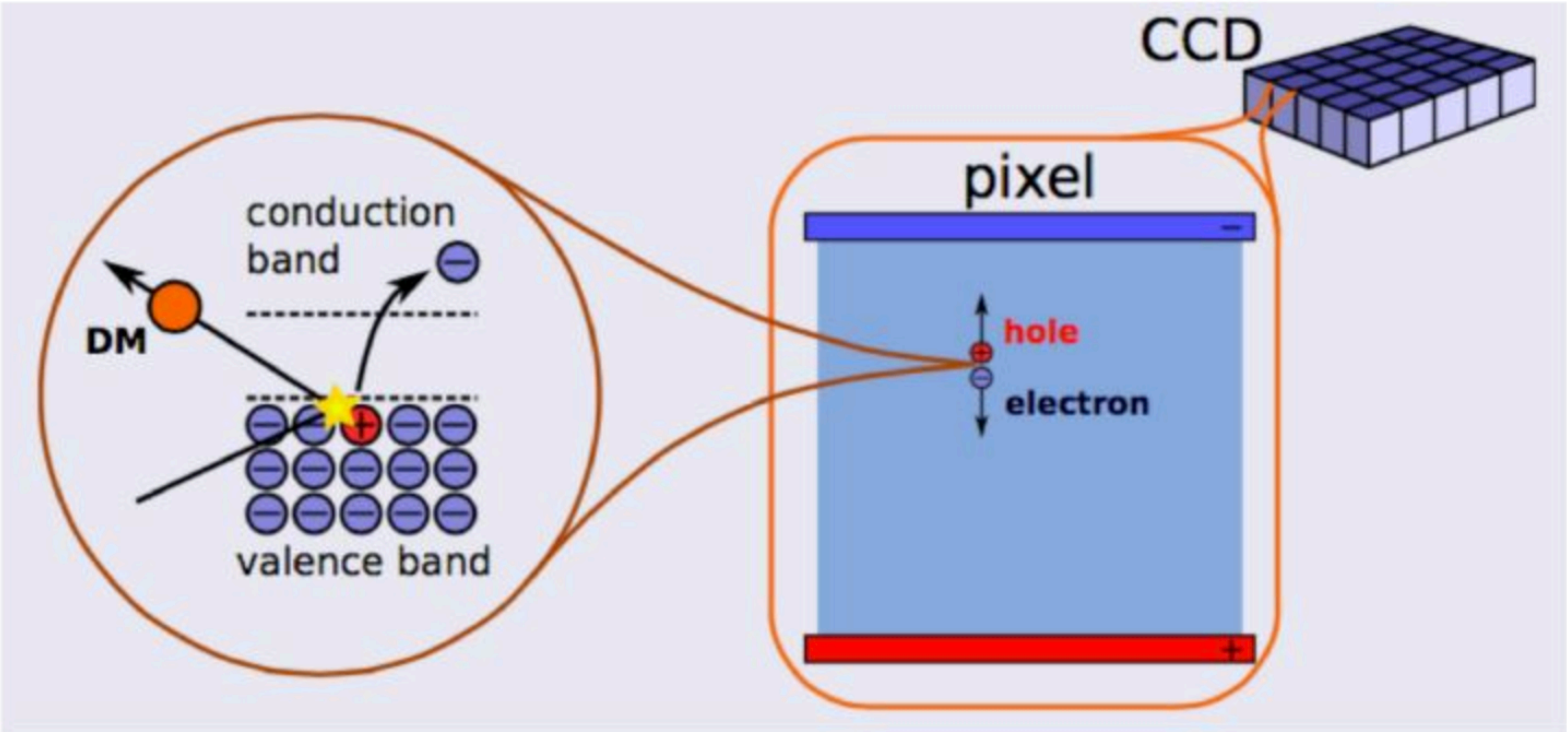

Yonit Hochberg

Charge only

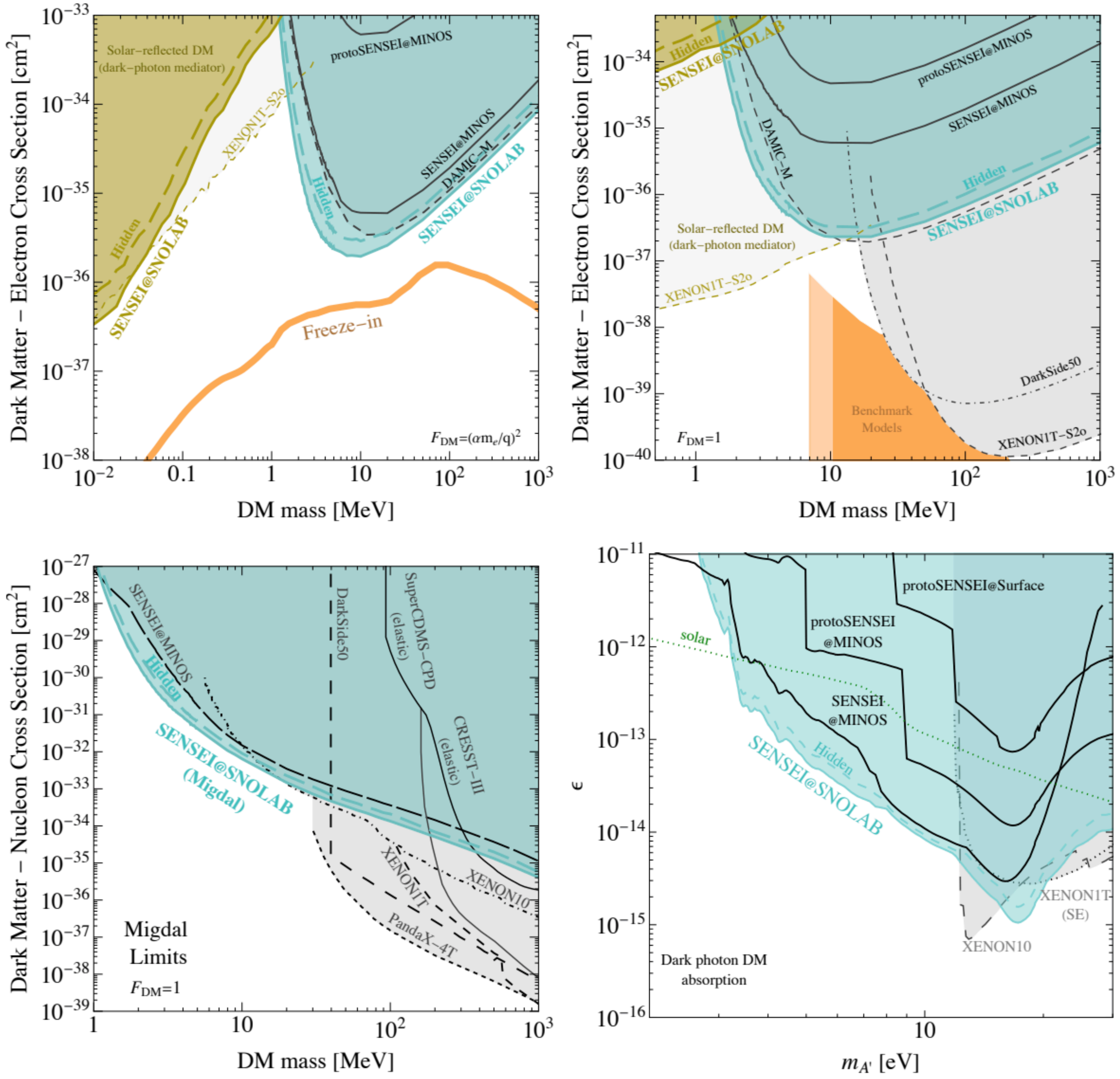

SENSEI@SNOLAB $E_{\rm th} \sim$ eV

2312.13342

Coincidence Cosmic Muons

2402.04245

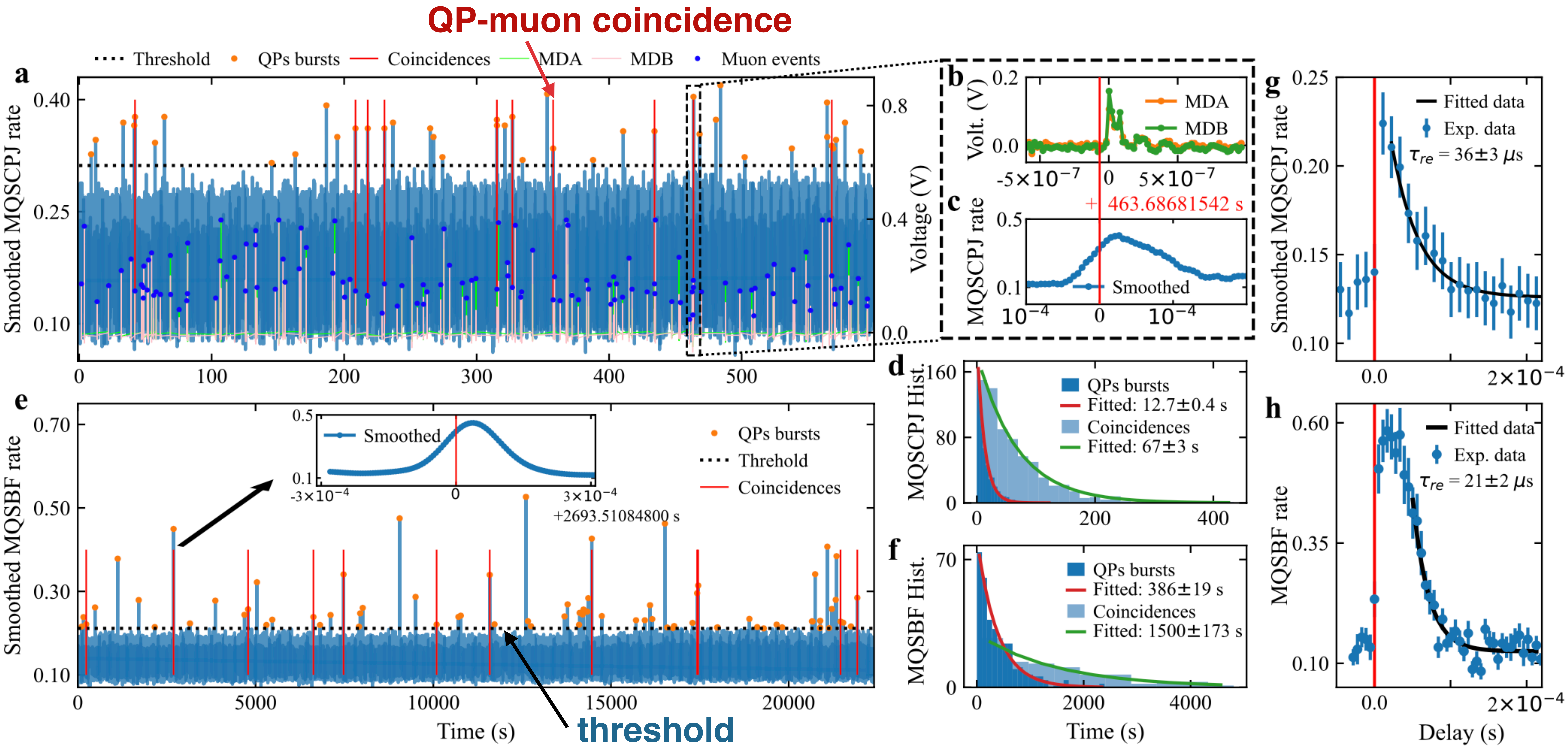

Signals at Qubit Arrays: Spin Flips

1106.0829

2402.04245

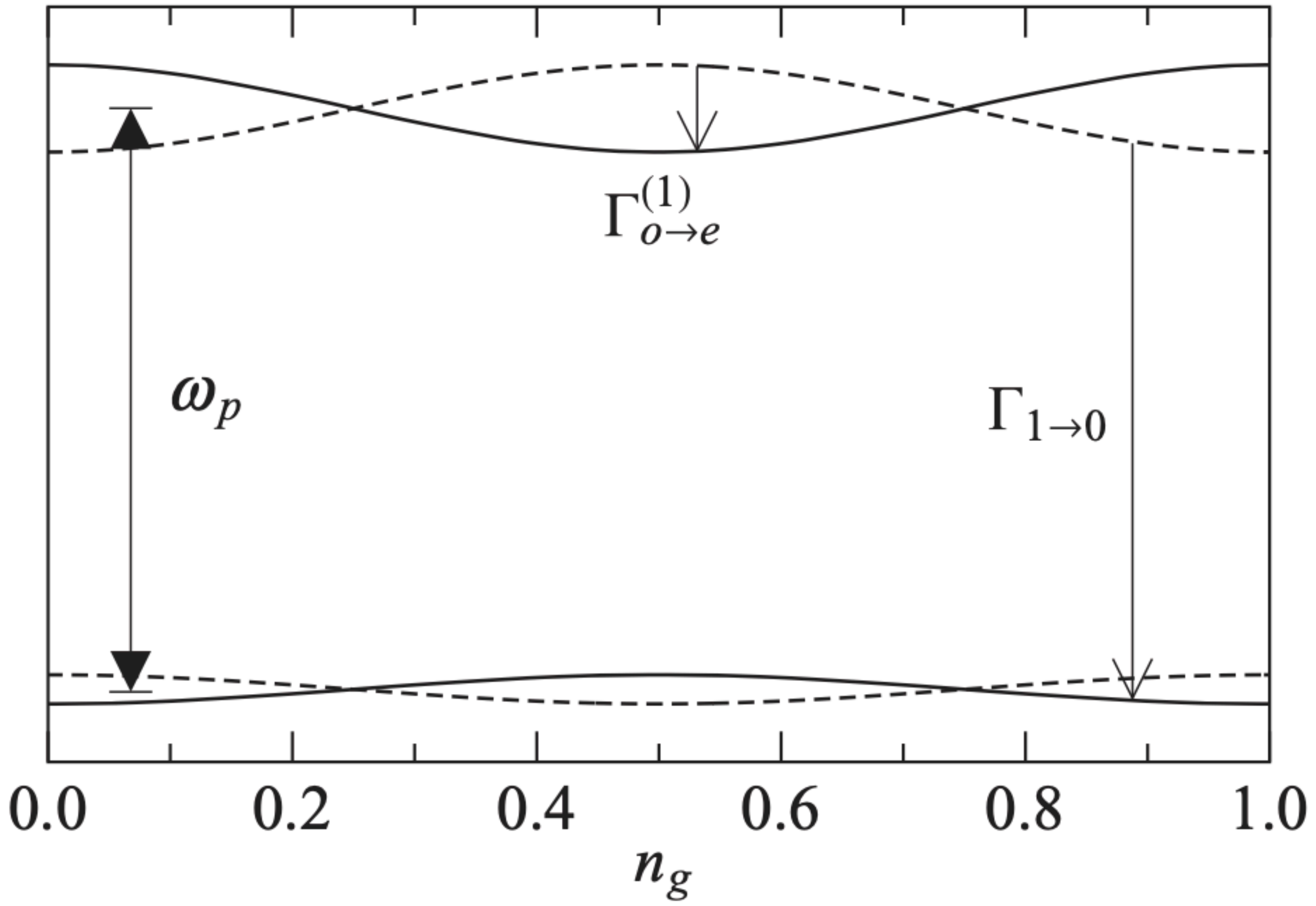

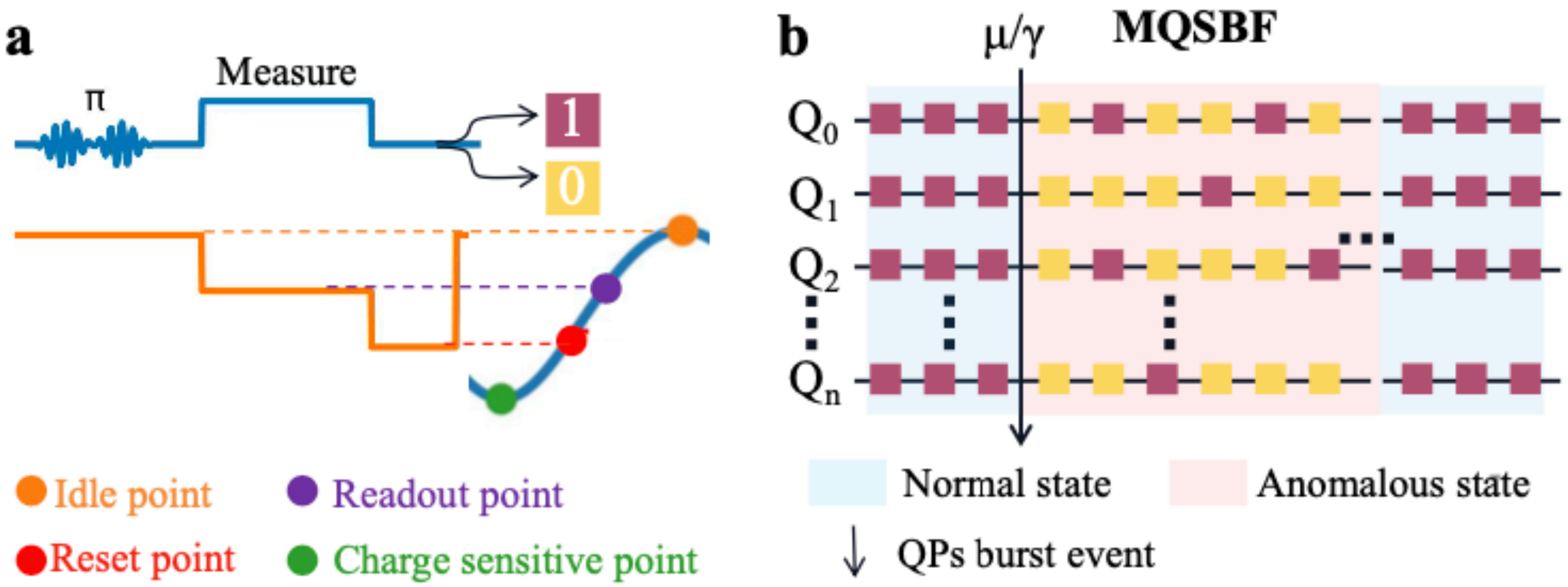

Change in qubit eigen states due to quasiparticle tunnelling

Quasiparticle Tunneling

2405.17192 **Charge-parity jumps**

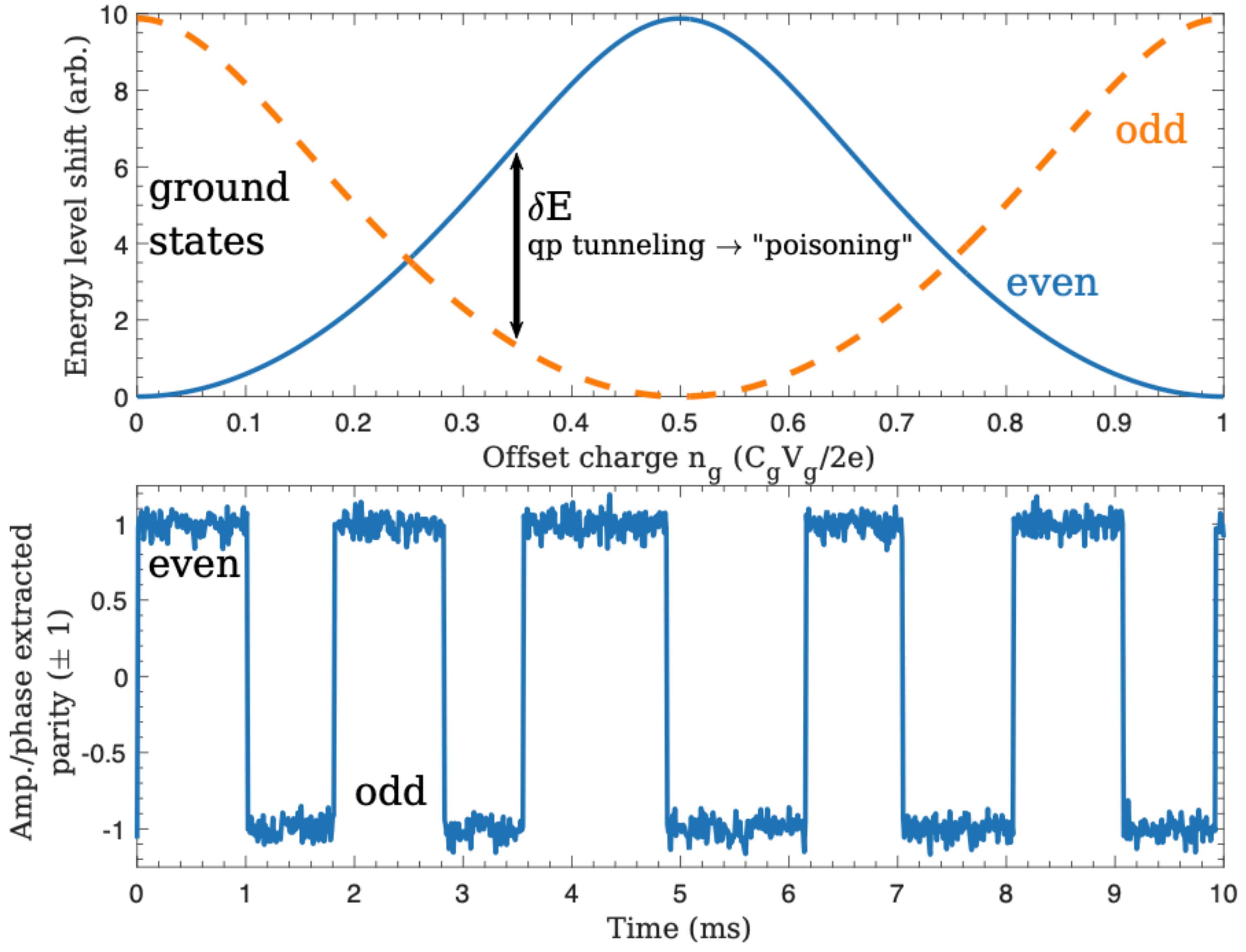

2402.04245

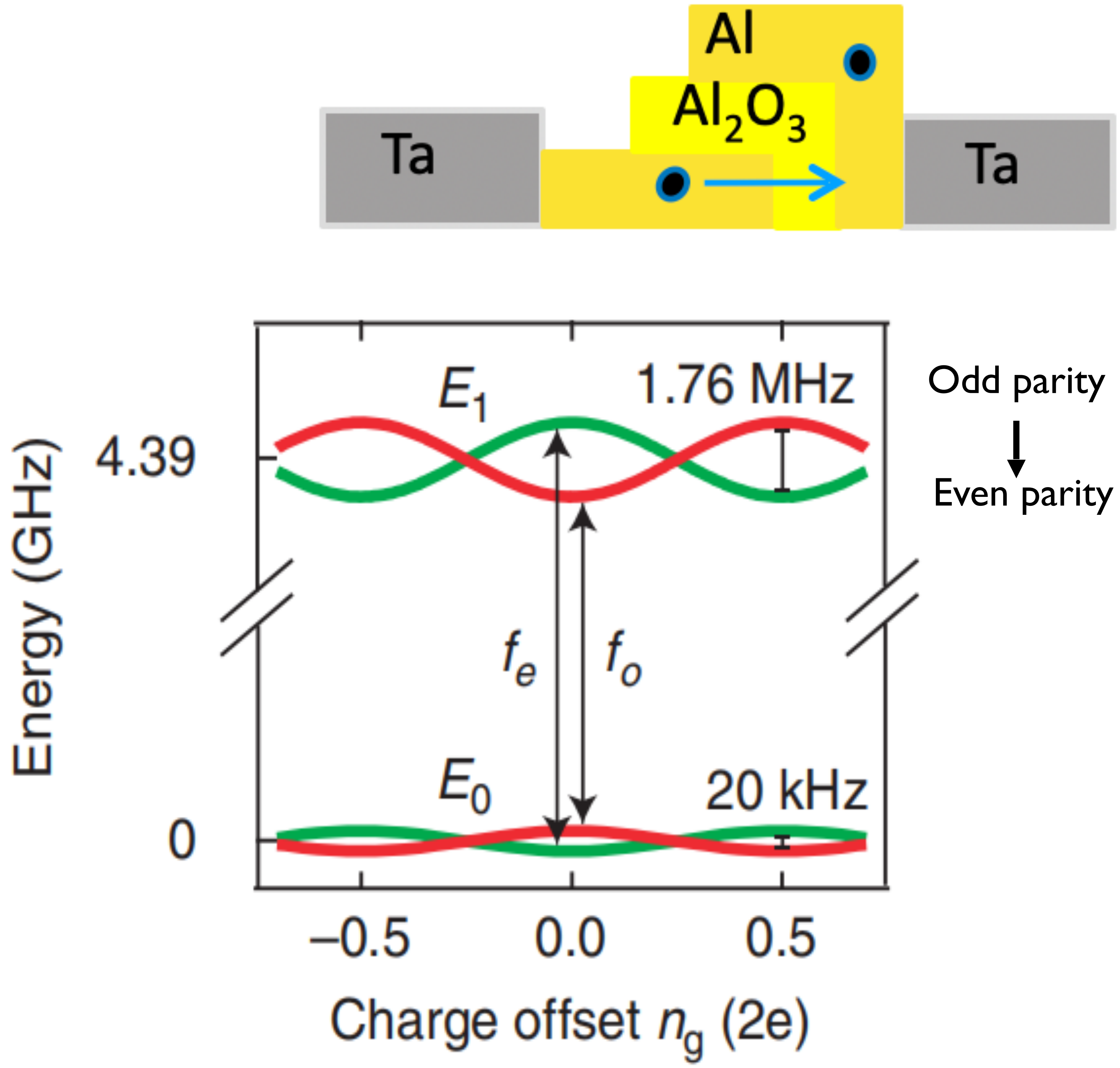

Charge parity change due to quasiparticle tunnelling

$\delta\mu \propto \mathrm{Log}[E_{\mathrm{phonon}}]$ ➡ $$\Gamma = \frac{16E_J}{h\Delta}\int_{\Delta}^{\infty} dE \frac{E(E+\delta E)-\Delta^2}{\sqrt{\left(E^2-\Delta^2\right)\left[(E+\delta E)^2-\Delta^2\right]}} f(E-\delta\mu)$$

准粒子隧穿信号

$$\delta n_{qp}(t) = \frac{N_{qp}^r}{V} \frac{\tau_{qp}}{\tau_{abs} - \tau_{qp}} \left(e^{-t/\tau_{abs}} - e^{-t/\tau_{qp}} \right)$$

准粒子寿命

$$N_{qp}^r = \frac{\eta_{ph} E_{dep}}{\Delta} = \frac{E_{abs}}{\Delta},$$

声子能量

$$f_{ne}(\epsilon) = \frac{1}{1 + e^{(\epsilon - \delta\mu)/k_B T}}. \qquad \delta\mu \approx k_B T \ln\left[1 + \frac{n_{qp}}{\mathcal{N}} e^{\Delta/k_B T}\right],$$

约瑟夫森能

隧穿前后能级差

$$\Gamma_{in} = \frac{16 E_J}{h\Delta} \int_{\Delta}^{\infty} dE \frac{E(E + \delta E) - \Delta^2}{\sqrt{(E^2 - \Delta^2)[(E + \delta E)^2 - \Delta^2]}} \times f(E - \delta\mu_{abs})[1 - f(E + \delta E - \delta\mu_{island})],$$

准粒子在超导膜中快速达到热平衡，产生化学势，使原本的费米-狄拉克分布产生偏离

Residual Quasiparticles

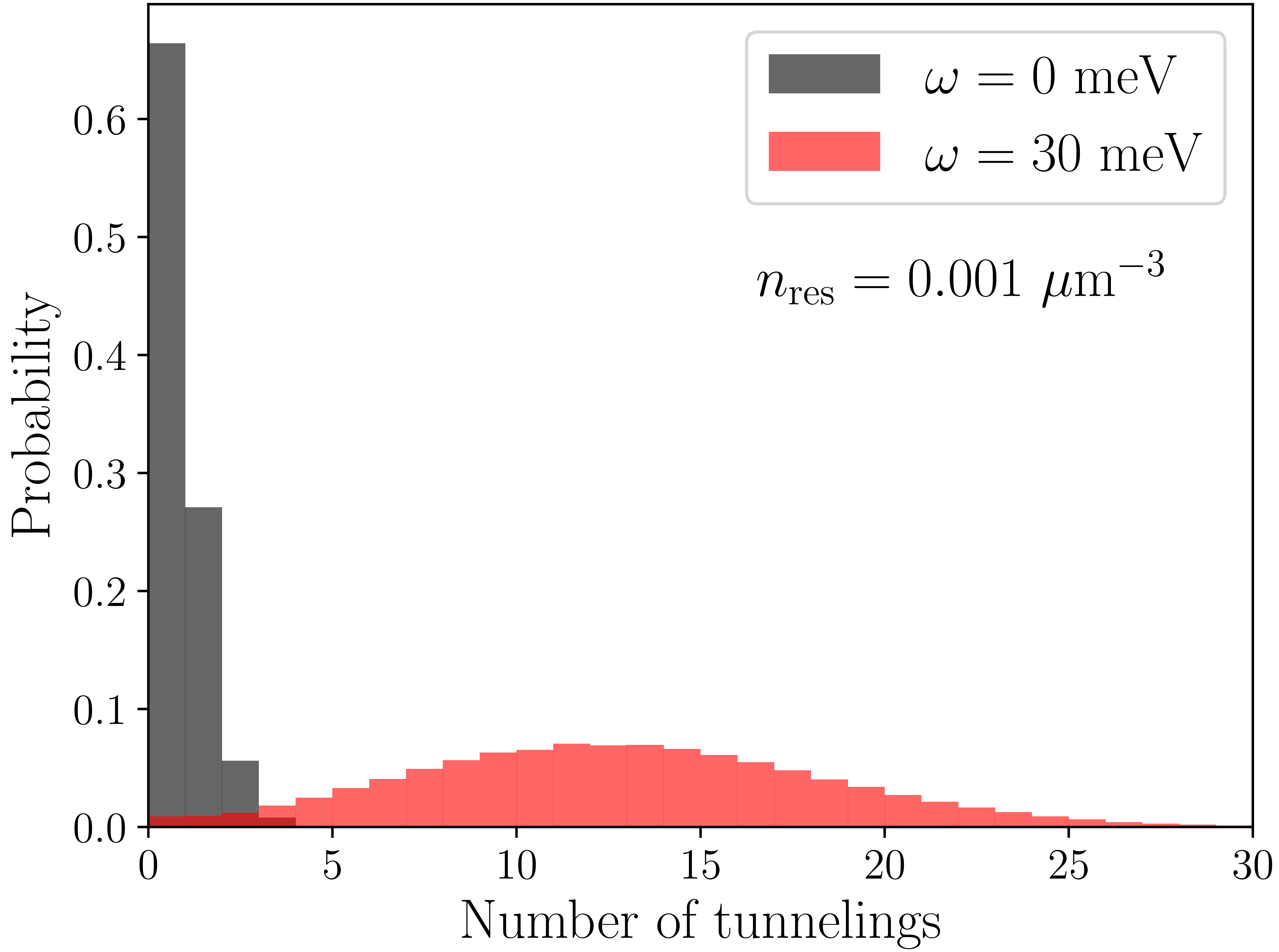

- Residual quasiparticles exist in the absence of a signal
- Distinguish signals from background based on the number of tunnelings

Efficiency and Threshold

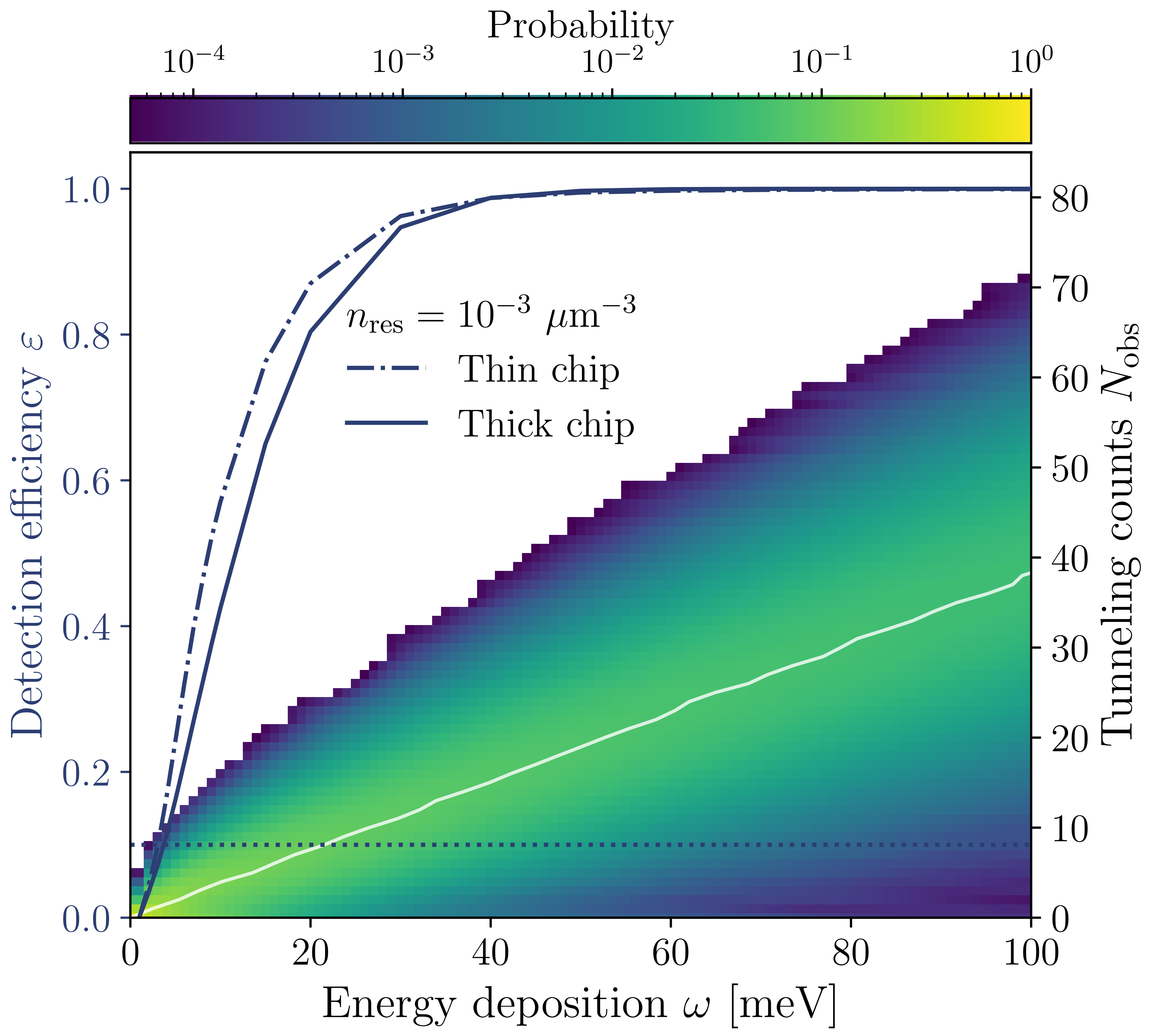

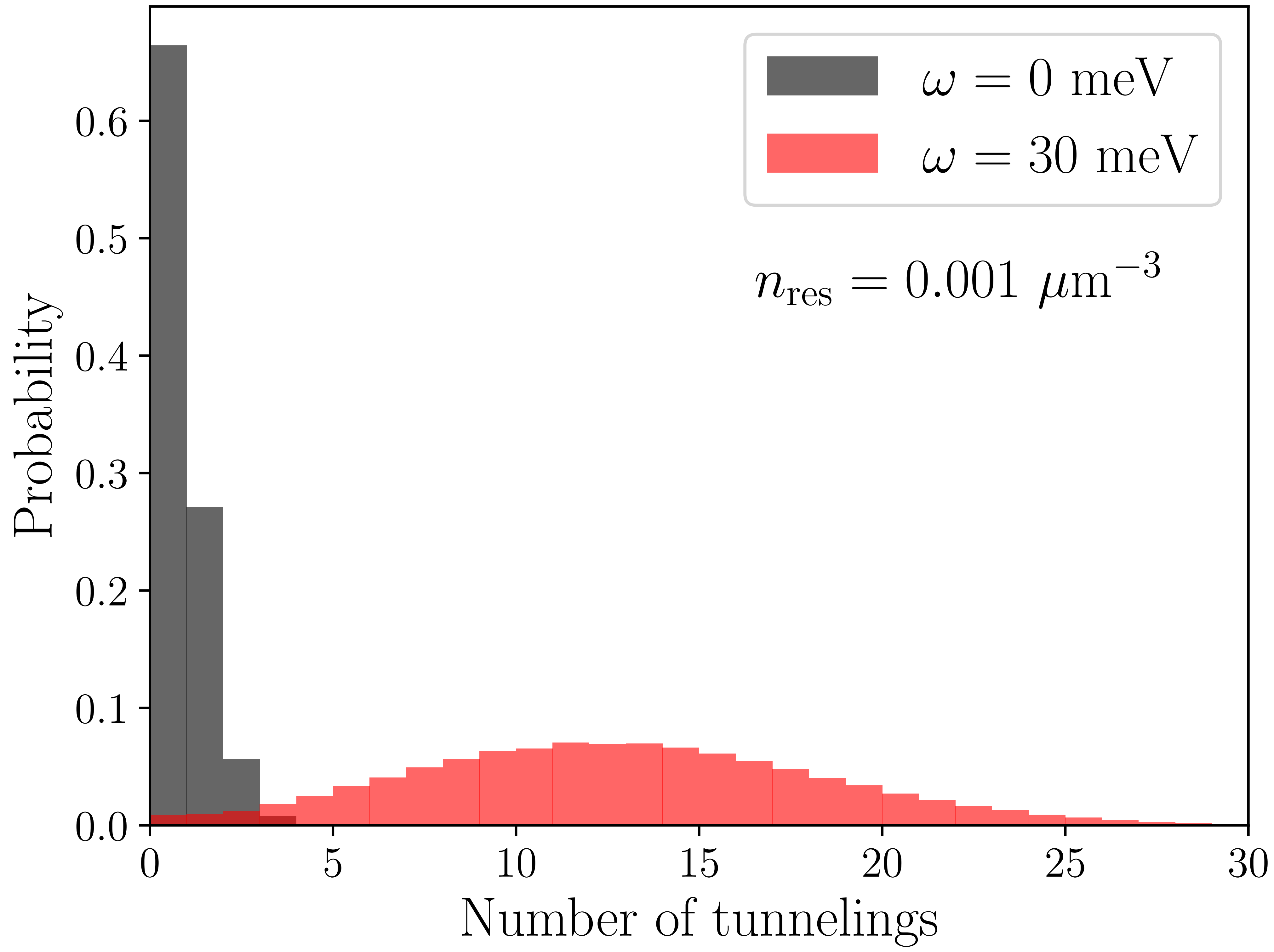

- Residual quasiparticles exist in the absence of a signal
- Distinguish signals from background based on the number of tunnelings
- $< 20\mathrm{meV}$ threshold could be achieved

Energy Resolution

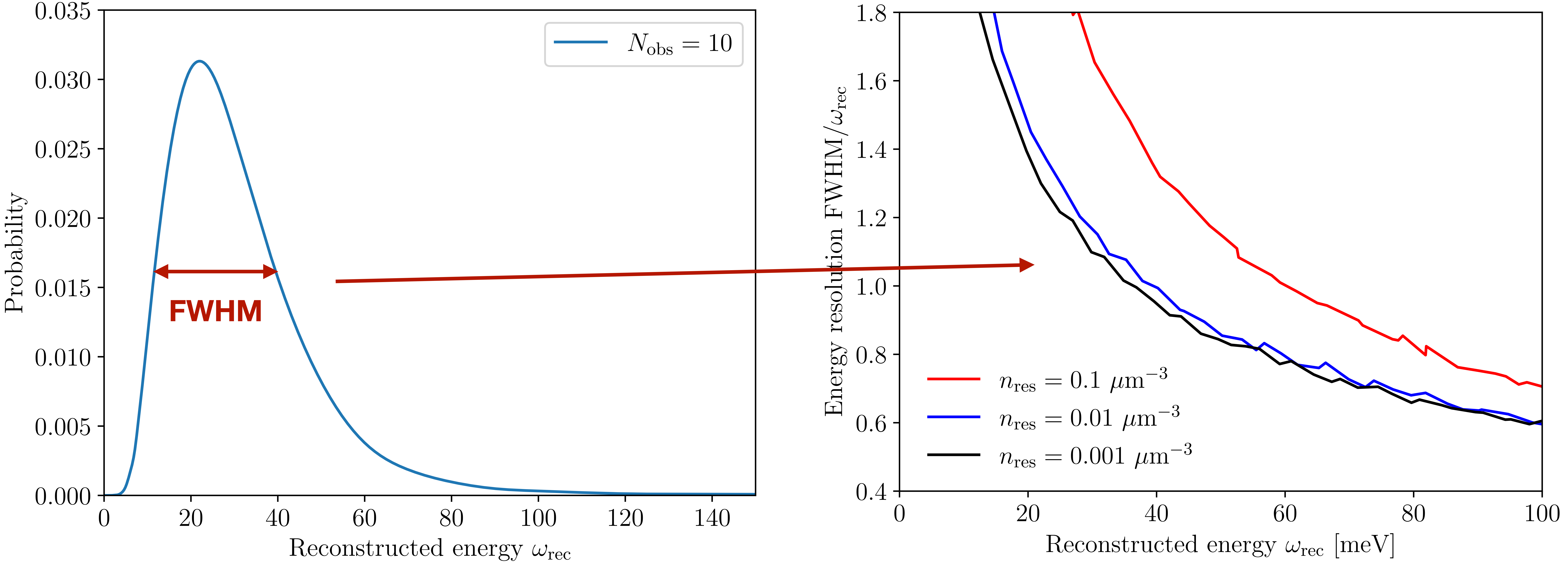

FWHM $= 2.355\sigma$

Small vs Large Detector

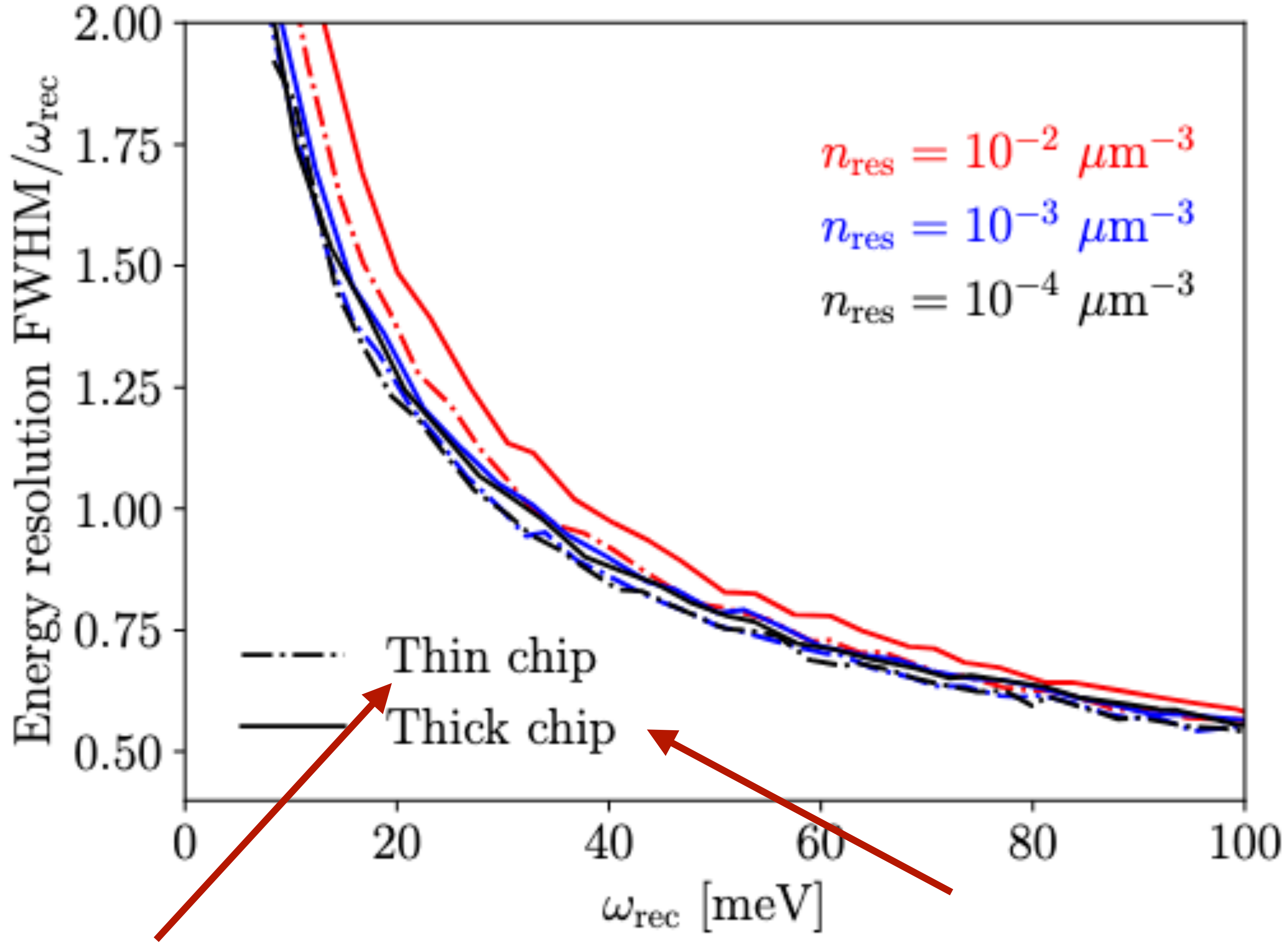

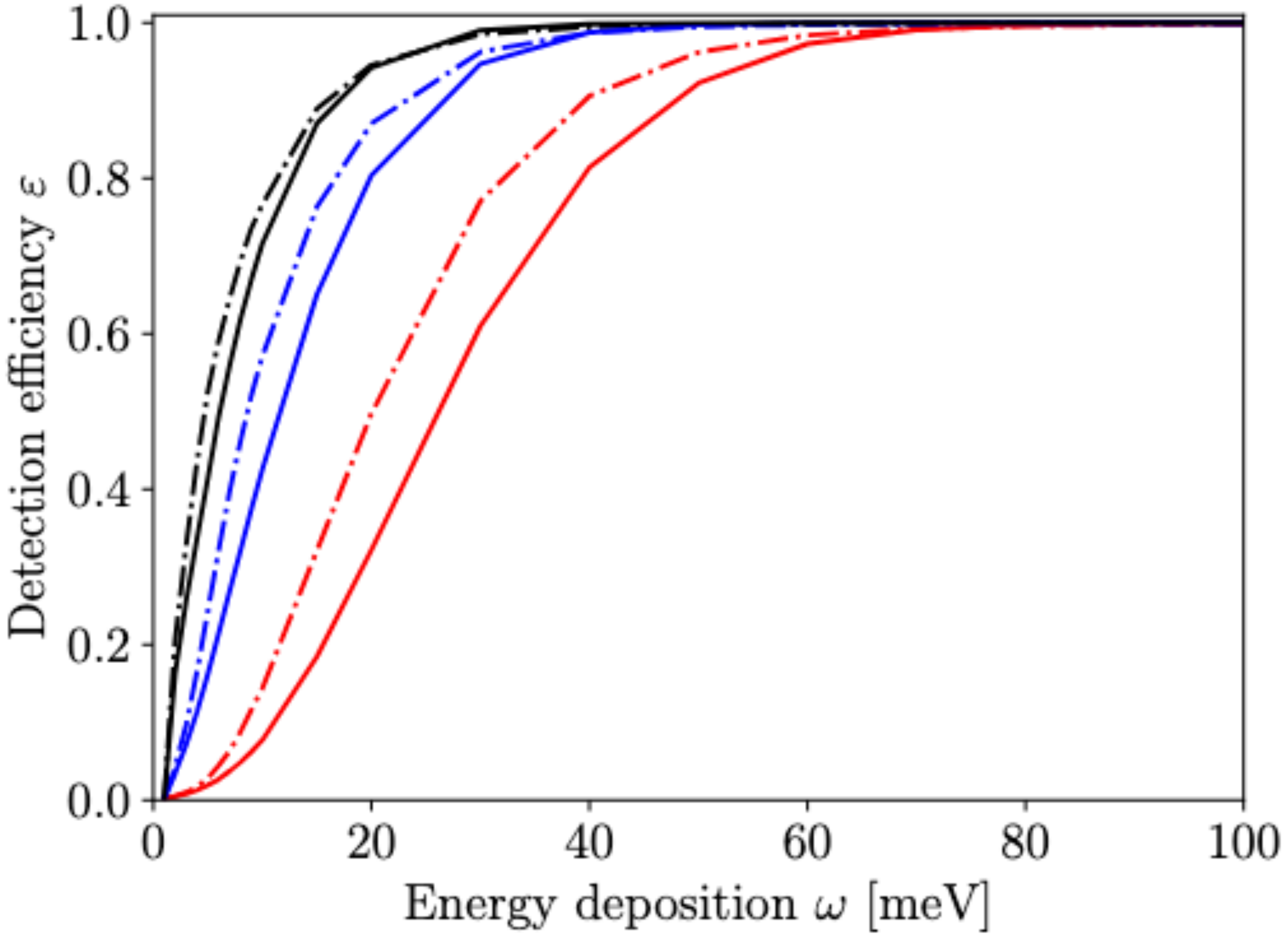

$20 \times 20 \times 0.43$ mm, 0.83 g

$20 \times 20 \times 20$ mm, 38 g

Phonon Propagation

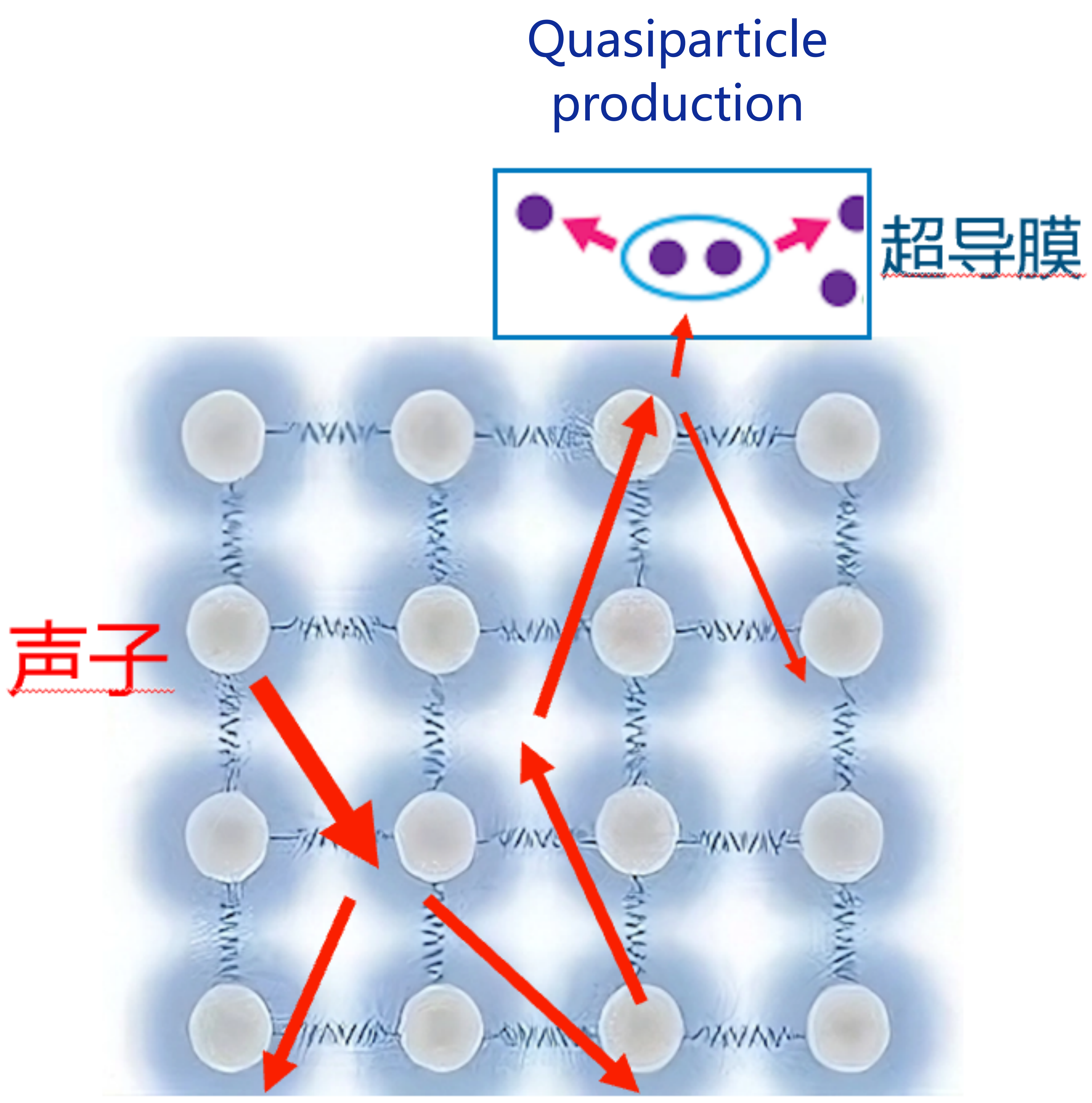

2302.05998

- Anharmonic down-conversion of longitudinal phonon
- Isotopic scattering of transverse phonon
- Reflection or absorption at the boundary/ interface, where absorption breaks Cooper pair and produces quasiparticles
- Mode change in scattering and reflection

$$\Gamma_{\mathrm{anh}} = A\nu^5,$$

$$\Gamma_{\mathrm{scatter}} = B\nu^4,$$

Quasiparticle Trapping

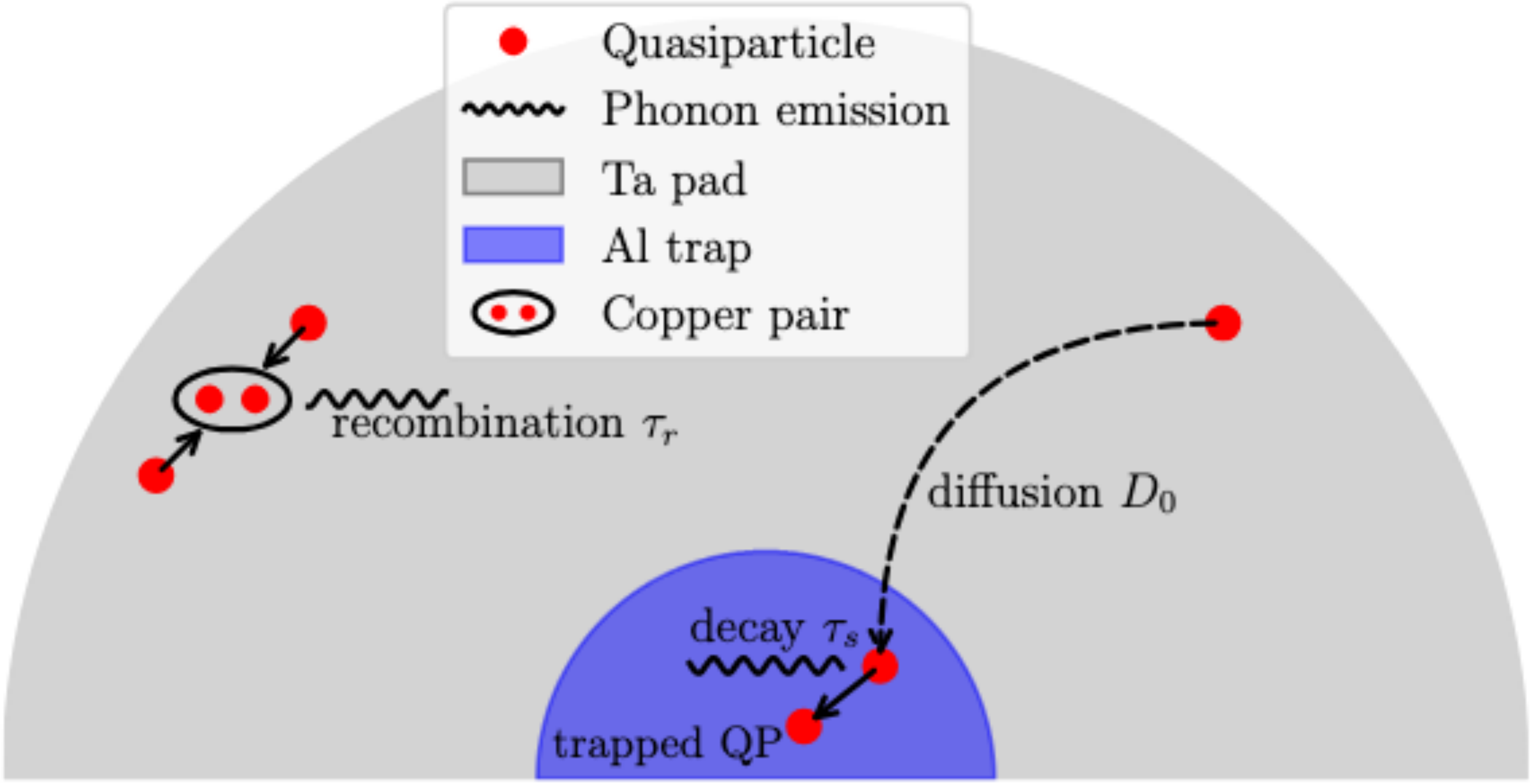

- Quasiparitcles diffuse from the higher gap Ta film to the lower gap Al film

- The quasiparticle number density in Al film is enhanced

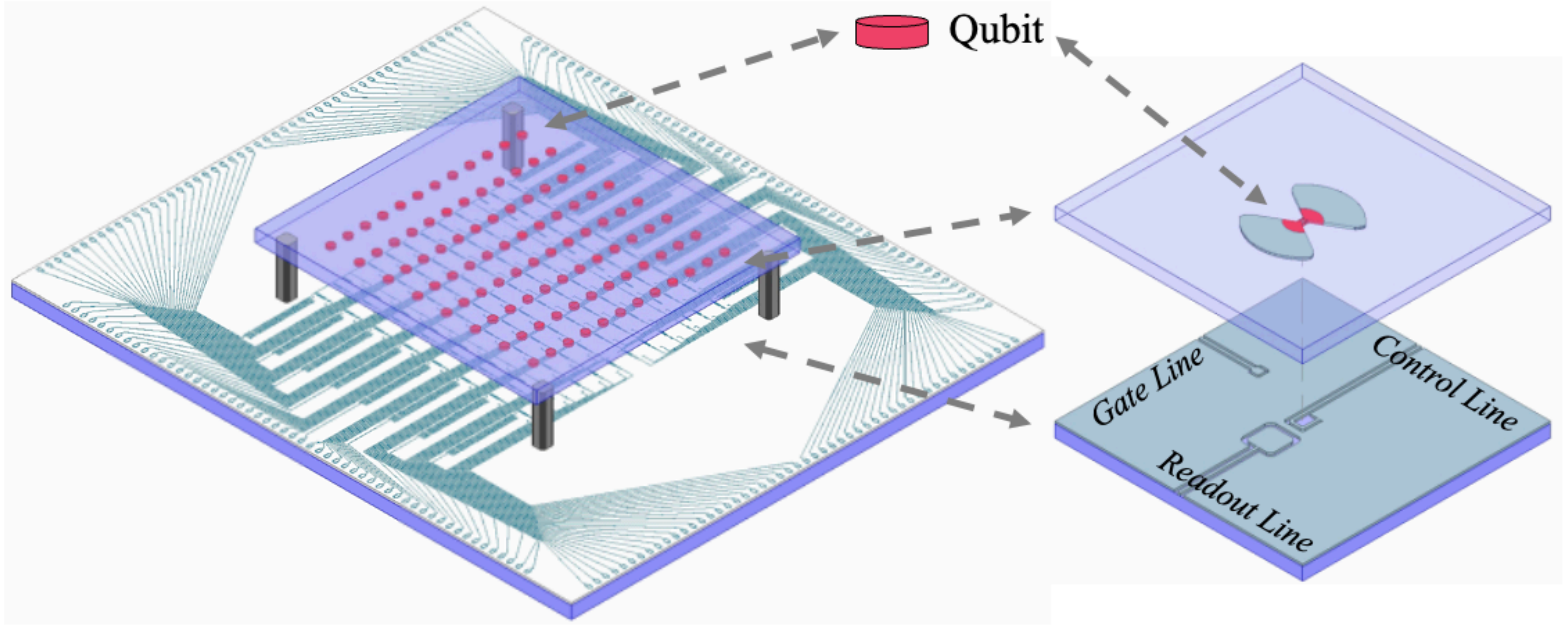

- **96 qubits to enhance phonon collection efficiency**
- **Separate the Qubit chip from the Carrier chip to minimize energy dissipation**

Quasiparticle Trapping

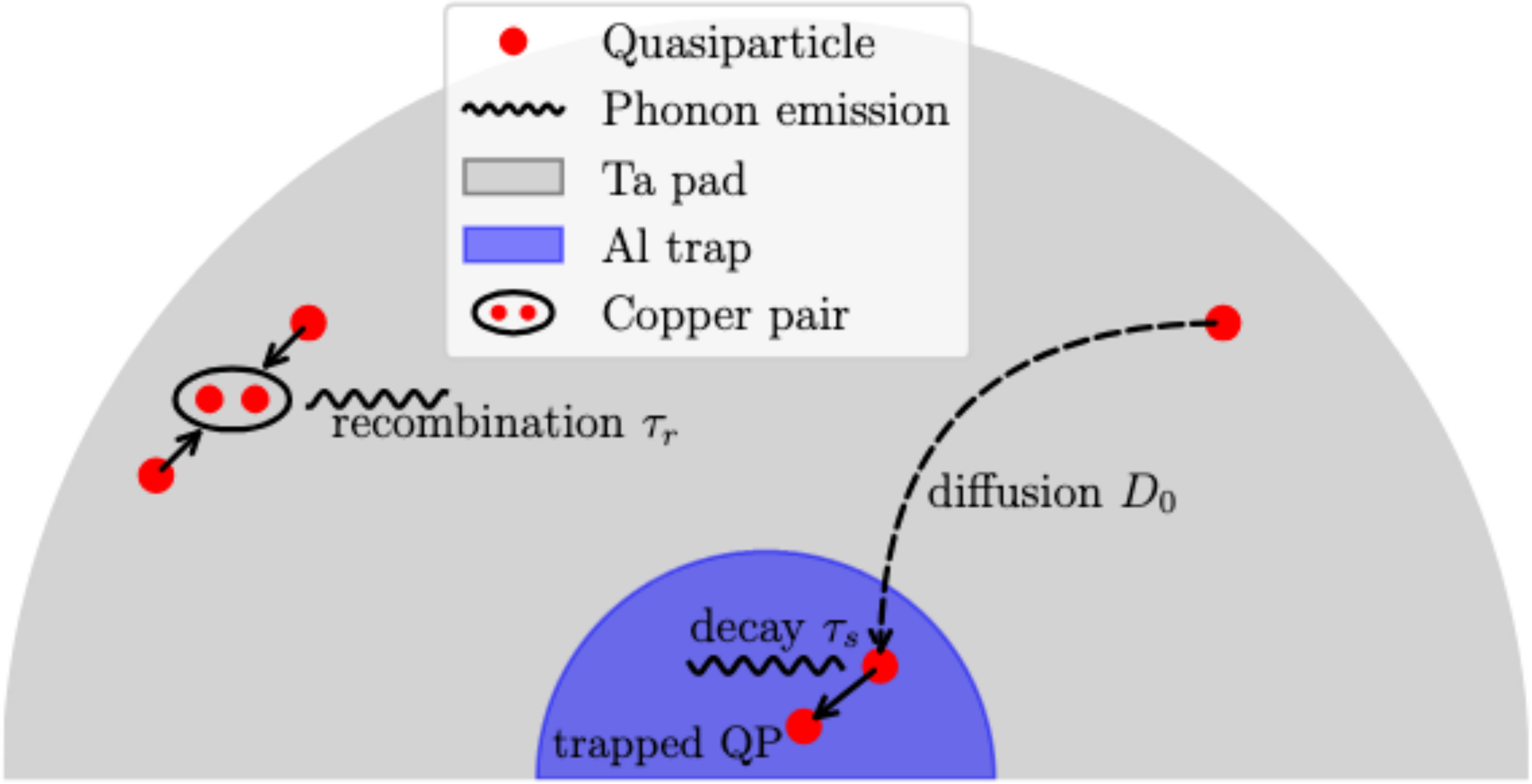

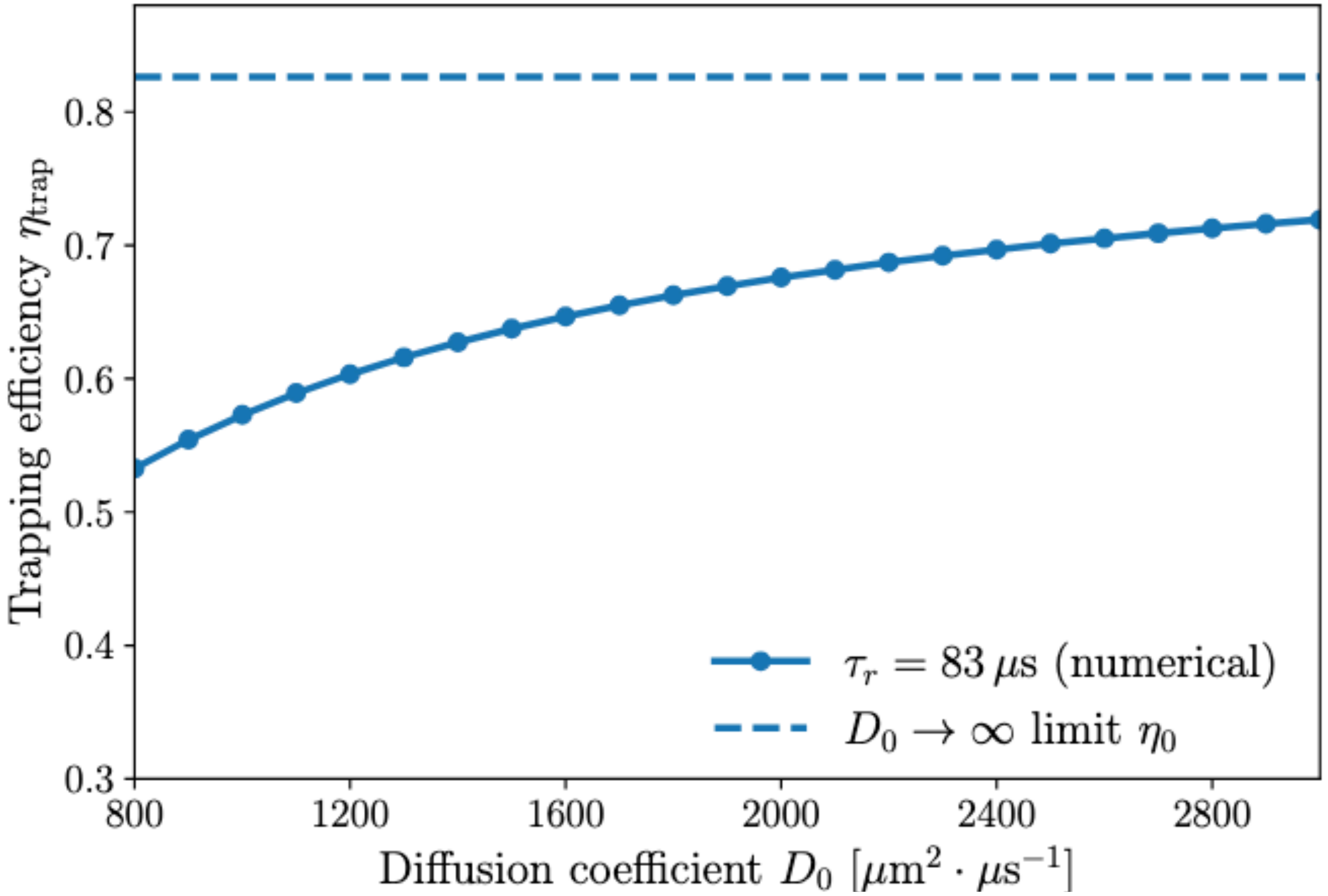

- Quasiparitcles diffuse from the higher gap Ta film to the lower gap Al film
- The quasiparticle number density in Al film is enhanced

$$\frac{\partial n(\boldsymbol{r},t)}{\partial t} = D_0 \nabla^2 n(\boldsymbol{r},t) - \frac{n(\boldsymbol{r},t)}{\tau(r^2)} + s(\boldsymbol{r},t)$$

diffusion coefficient

quasiparticle recombination

source

Quantum Parity Measurements

Charge-parity jumps

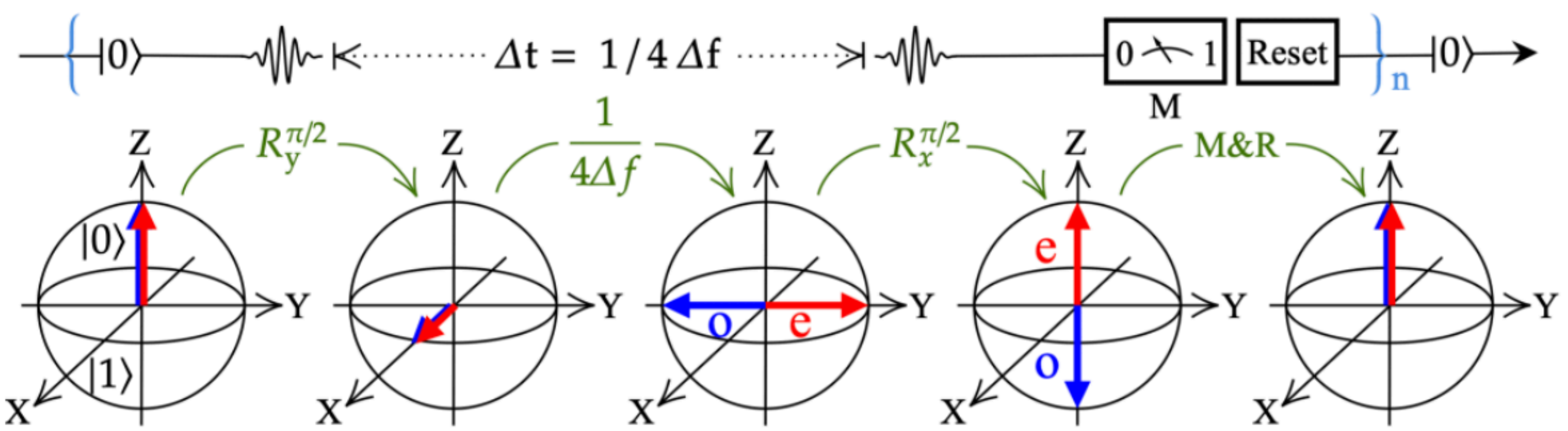

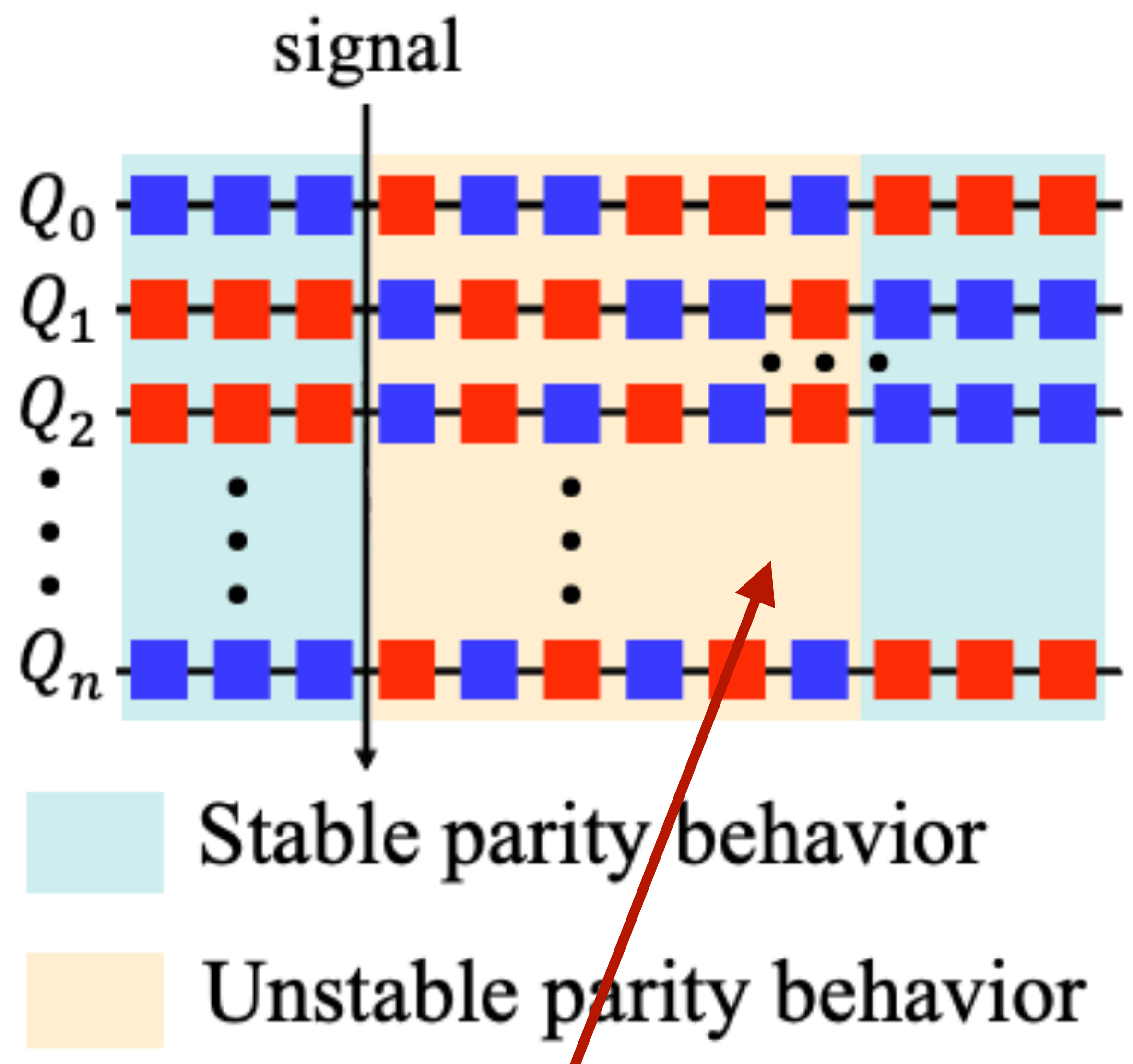

Dark matter incident

- When dark matter scatters, multiple qubits exhibit parity switches
- Measure the number of tunnelings in all qubits as a proxy of energy deposition

Quasiparticle Tunnelling

2405.17192 **Charge-parity jumps**

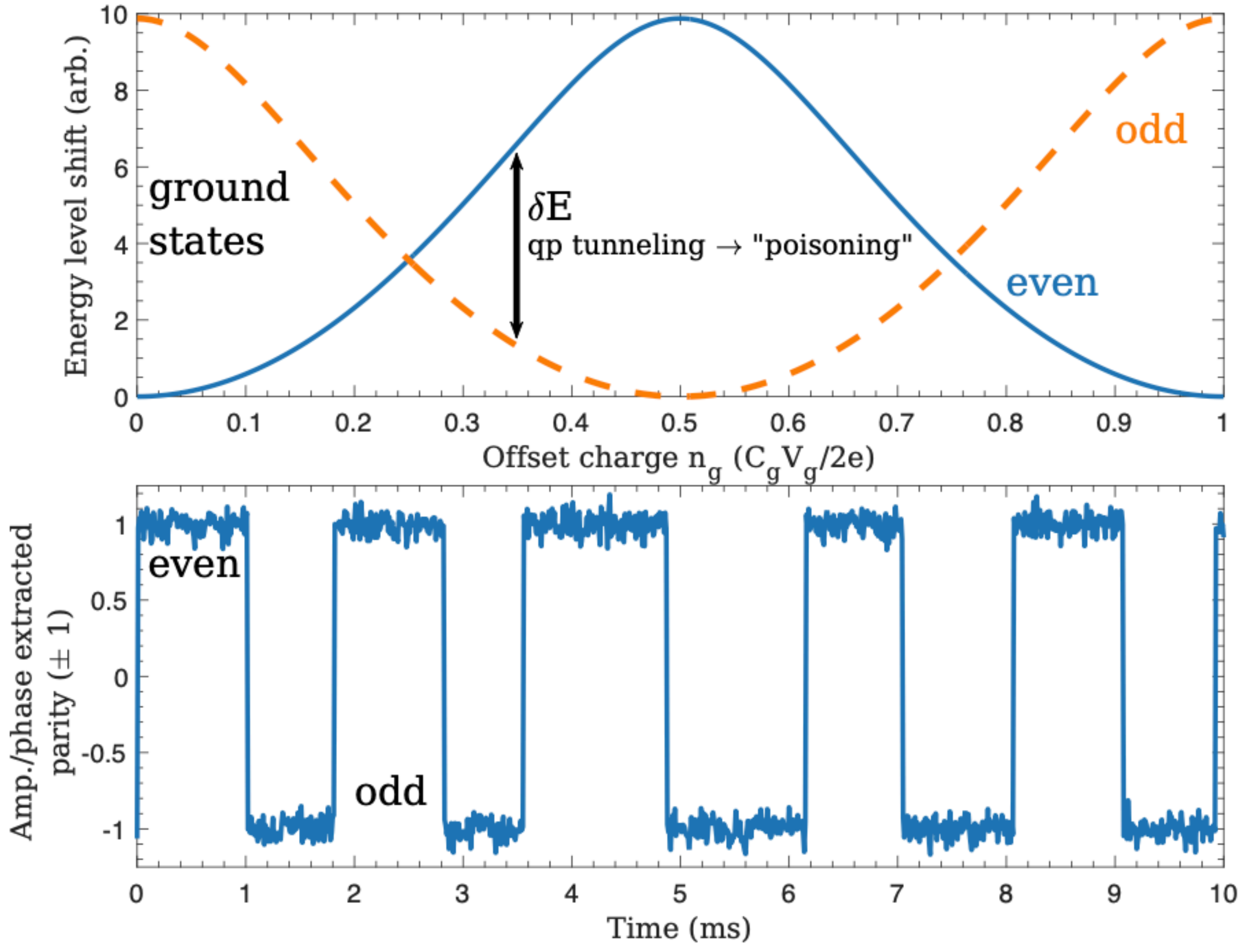

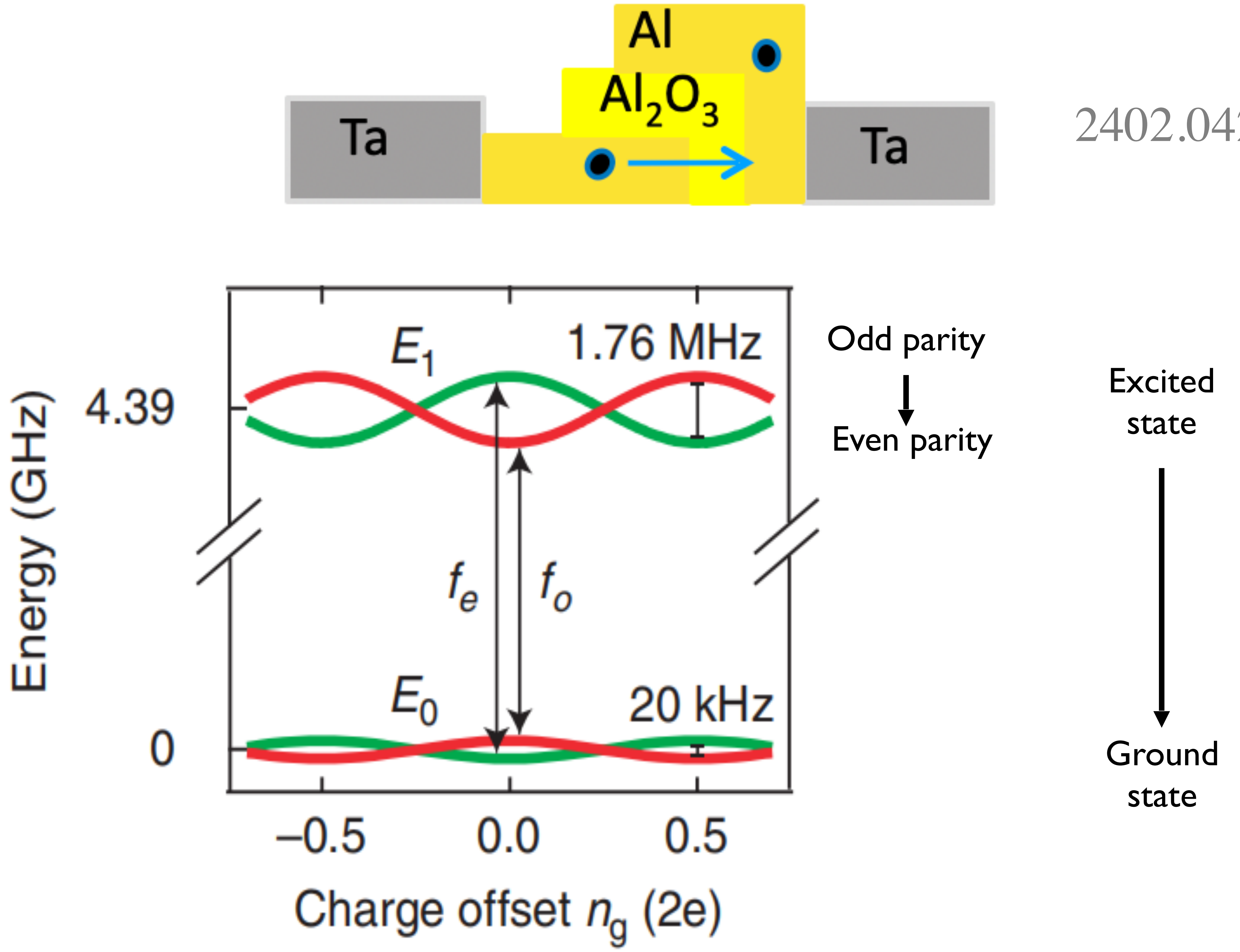

2402.04245

Charge parity change due to quasiparticle tunnelling

Quasiparticle Tunnelling Rate

$$\delta n_{qp}(t) = \frac{N_{qp}^r}{V} \frac{\tau_{qp}}{\tau_{abs} - \tau_{qp}} \left(e^{-t/\tau_{abs}} - e^{-t/\tau_{qp}} \right)$$

quasiparticle lifetime

$$N_{qp}^r = \frac{\eta_{ph} E_{dep}}{\Delta} = \frac{E_{abs}}{\Delta},$$

phonon energy

$$f_{ne}(\epsilon) = \frac{1}{1 + e^{(\epsilon - \delta\mu)/k_B T}}. \qquad \delta\mu \approx k_B T \ln\left[1 + \frac{n_{qp}}{\mathcal{N}} e^{\Delta/k_B T}\right],$$

$$\delta\mu \propto \mathrm{Log}[E_{phonon}]$$

Josephson energy

energy difference after tunneling

$$\Gamma_{in} = \frac{16 E_J}{h\Delta} \int_\Delta^\infty dE \frac{E(E+\delta E) - \Delta^2}{\sqrt{(E^2 - \Delta^2)[(E+\delta E)^2 - \Delta^2]}} \times f(E - \delta\mu_{abs})[1 - f(E + \delta E - \delta\mu_{island})],$$

$$\Gamma_{tun}(t) \simeq \frac{16 E_J k_B T}{h \mathcal{N}_{qp} \Delta_{trap}} n_{qp} e^{-t/\tau_{qp}} \qquad n_{qp} = \eta_{pb} \eta_{trap} E_{ph} / V_{trap} \Delta_{trap}$$

Quasiparticles quickly thermalize in the film, producing a shift in the chemical potential

Readout Errors

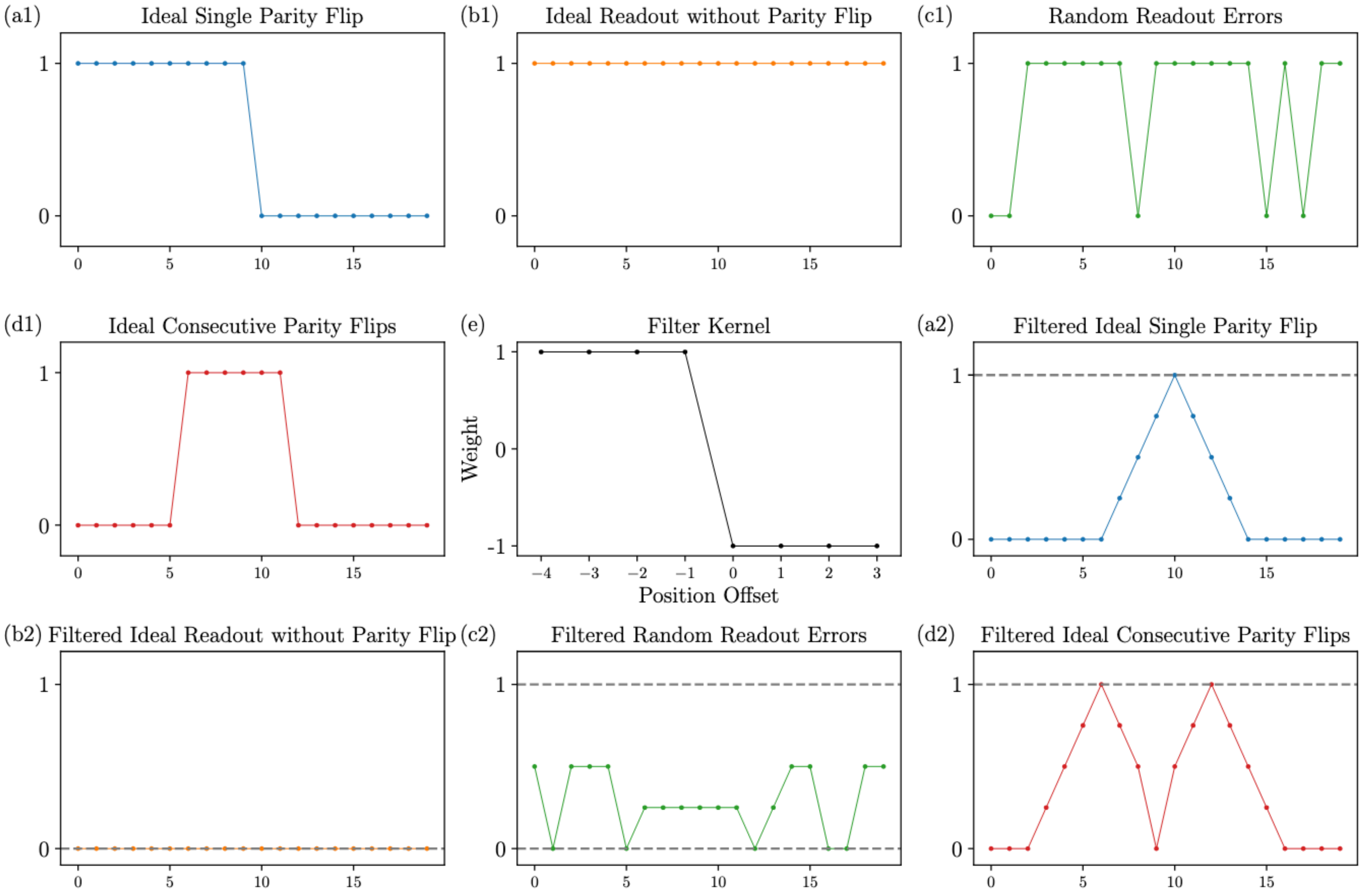

Readout error could randomly occur at a probability less than 5%

Readout Errors

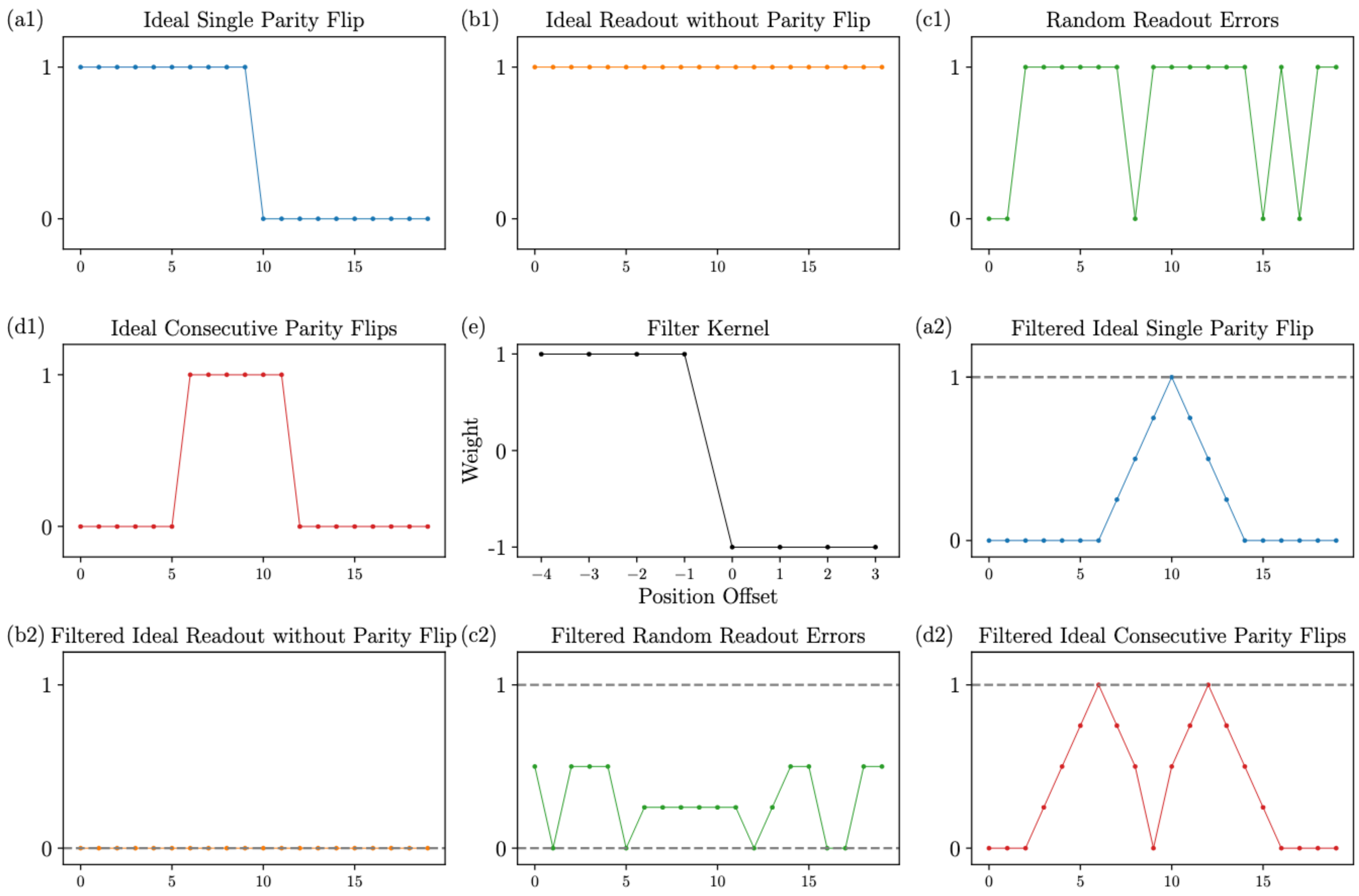

filter

$$h = [\underbrace{1, \ldots, 1}_{L}, \underbrace{-1, \ldots, -1}_{L}]$$

$$s'[k] = \frac{1}{L} \left| \sum_{i=0}^{2L-1} s[k+i-L]h[i] \right|$$

Apply a filter to distinguish tunnelling signal from random readout errors

Readout Errors

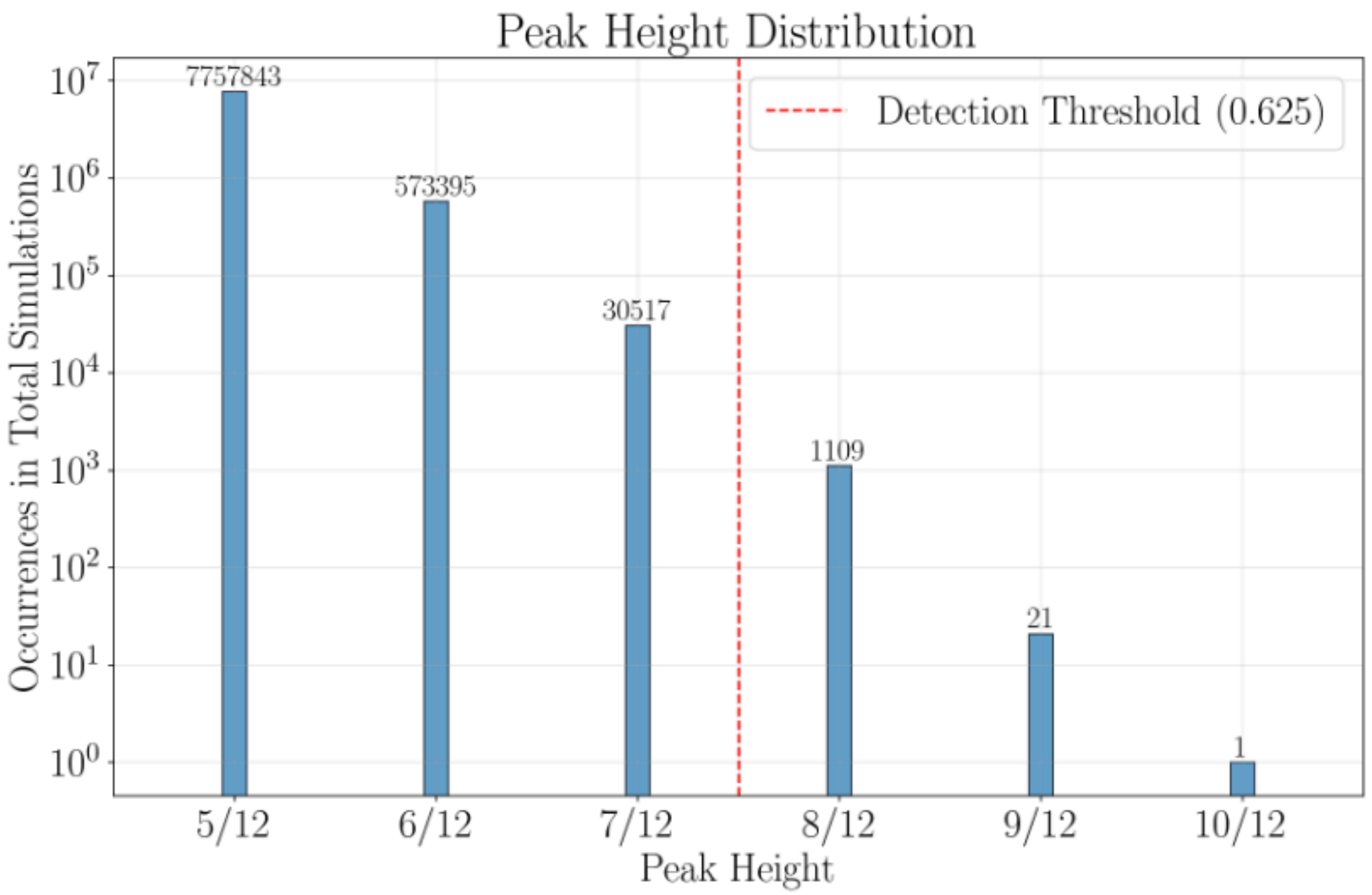

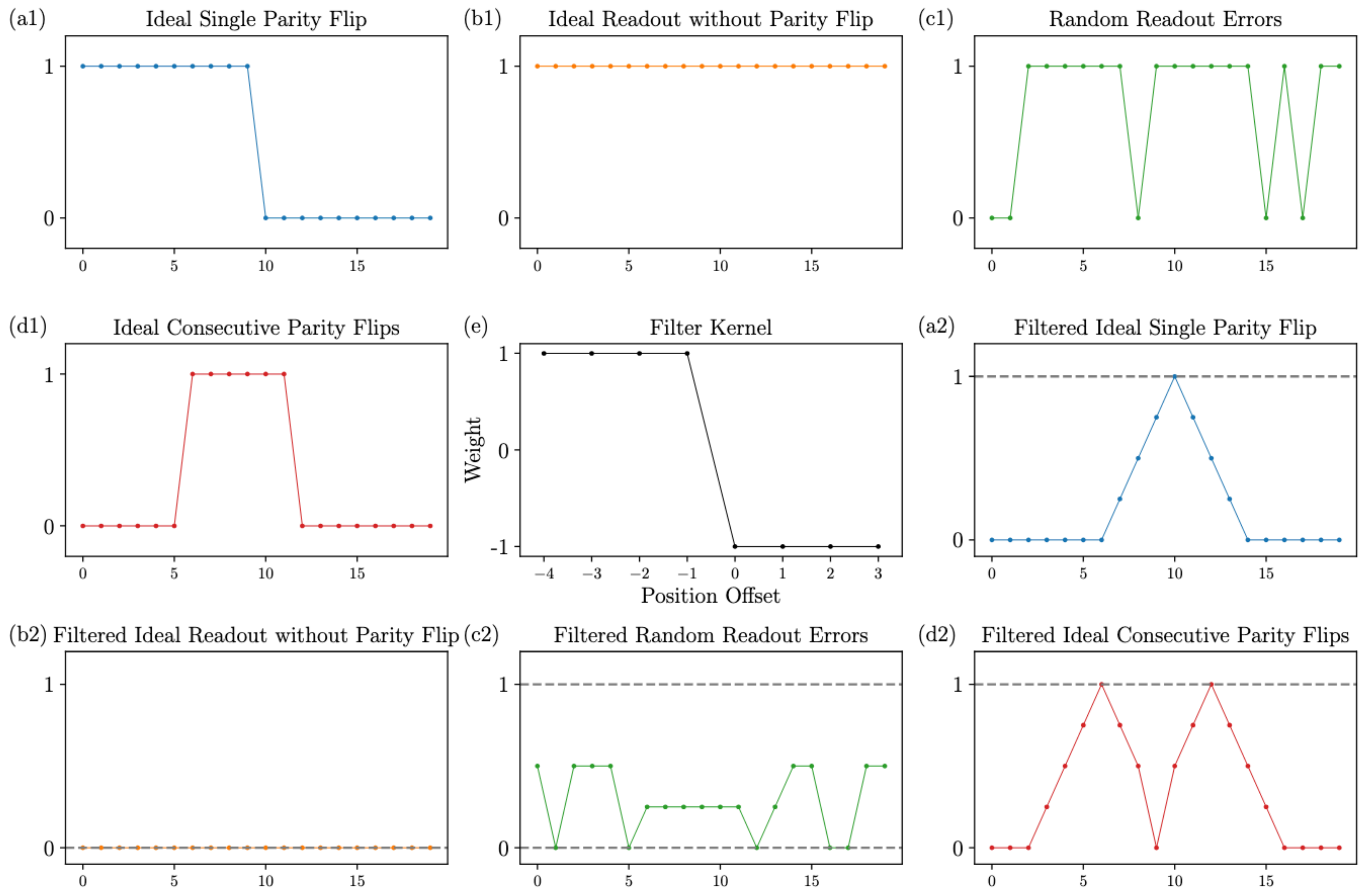

The false-positive rate is about 0.01 Hz after filtering, two orders of magnitude below the residual quasiparticle tunnelling rate

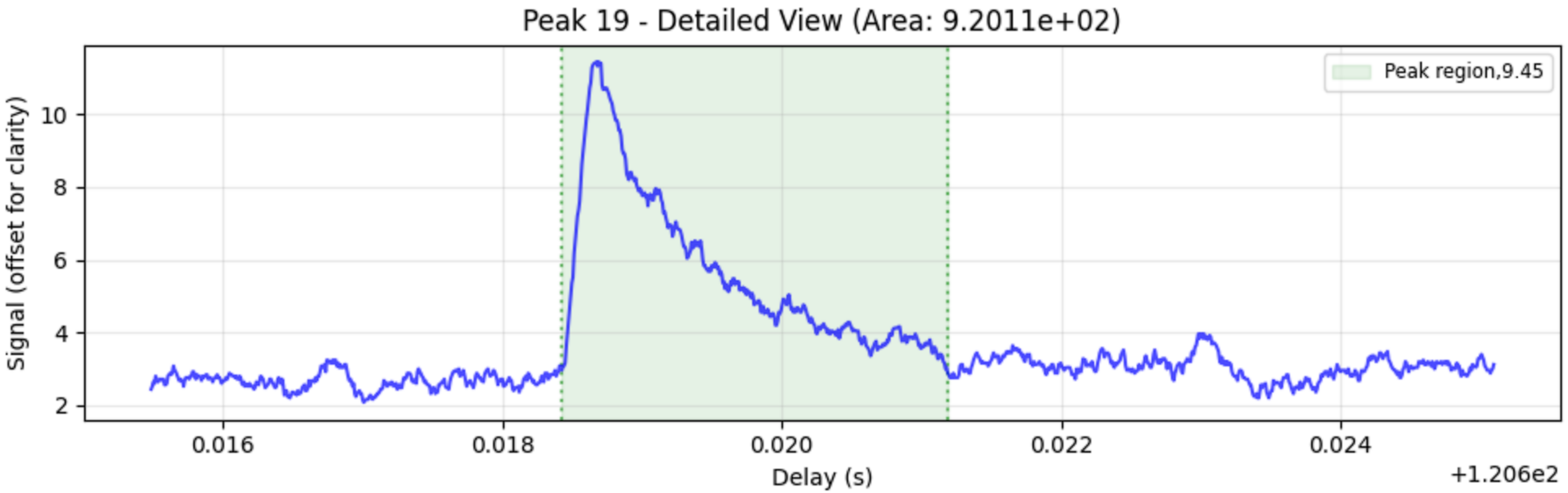
Peak 19 - Detailed View (Area: 9.2011e+02)
Peak region,9.45
Signal (offset for clarity)
Delay (s)
+1.206e2
0.016
0.018
0.020
0.022
0.024
2
4
6
8
10

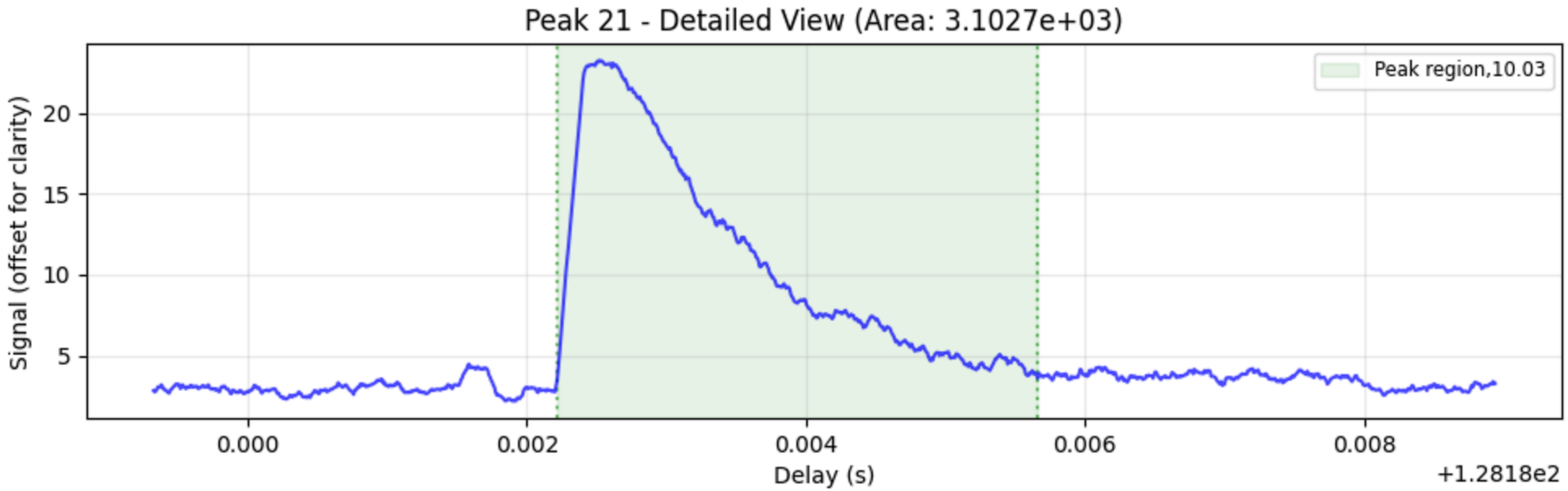
Peak 21 - Detailed View (Area: 3.1027e+03)
Peak region,10.03
Signal (offset for clarity)
Delay (s)
+1.2818e2
0.000
0.002
0.004
0.006
0.008
5
10
15
20

时间线和实验结果

- 25/11/22开始降温
- 25/12/30开始采集无屏蔽的环境背景数据
  - 有效测量时间372051.5 s (103.35 hrs)；阈值以上事件数25157，事件率67.62±0.43 mHz.
- 26/01/19开始采集有屏蔽的环境背景数据
  - 有效测量时间448354.3 s (124.54 hrs)；阈值以上事件数2443，事件率5.45±0.11 mHz.
- 26/01/29-01/30, 26/02/04至今采集有屏蔽+Cs-137放射源的数据
  - 目前有效测量时间87174.4 s (24.22 hrs)；阈值以上事件数3314，事件率38.02±0.66 mHz.

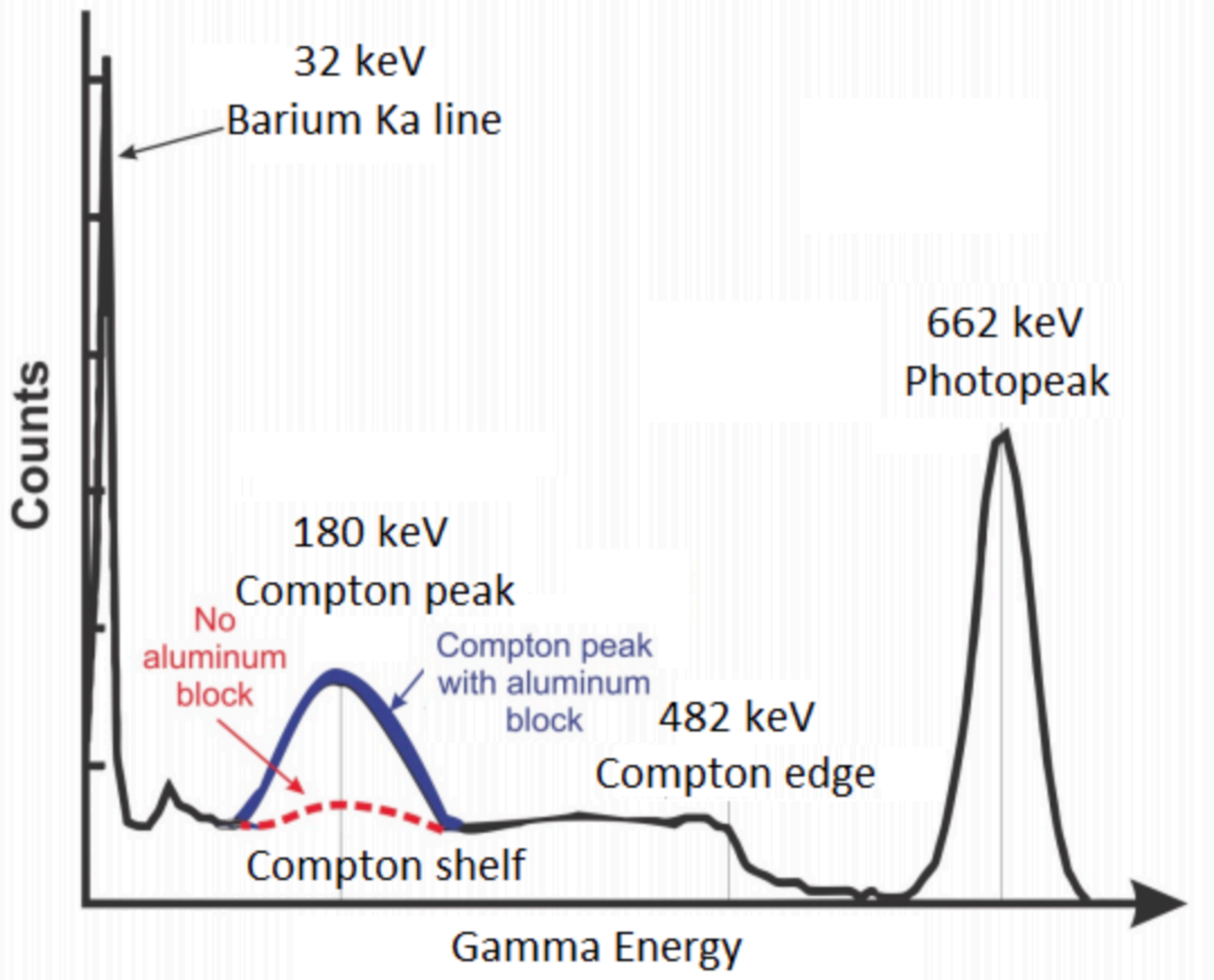

事件率与Geant4模拟差距百分之几，说明阈值对应的沉积能量在O(keV)

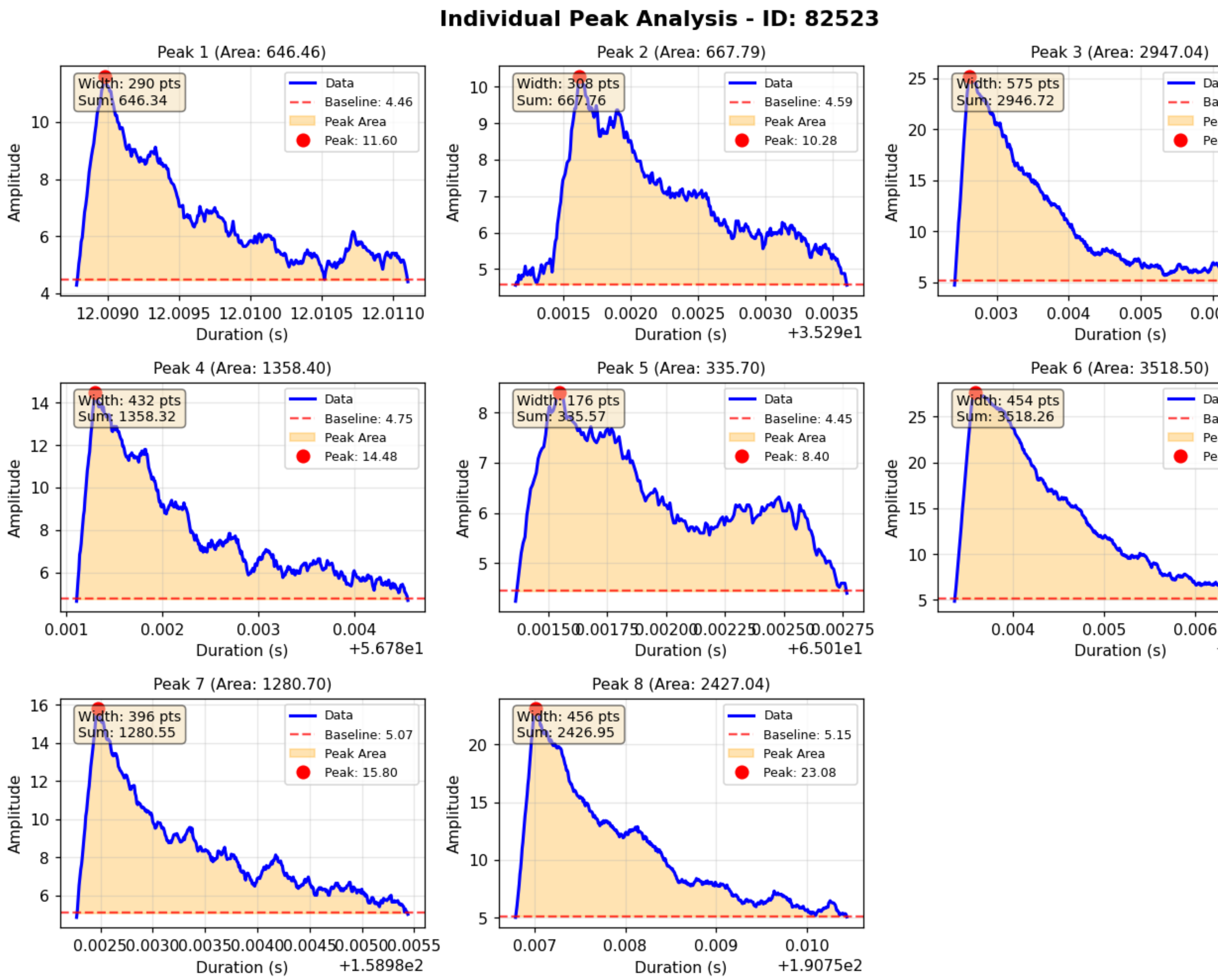

Individual Peak Analysis - ID: 82523
Peak 1 (Area: 646.46)
Width: 290 pts
Sum: 646.34
Data
Baseline: 4.46
Peak Area
Peak: 11.60
Peak 2 (Area: 667.79)
Width: 308 pts
Sum: 667.76
Baseline: 4.59
Peak: 10.28
Peak 3 (Area: 2947.04)
Width: 575 pts
Sum: 2946.72
Baseline: 5.18
Peak: 25.16
Peak 4 (Area: 1358.40)
Width: 432 pts
Sum: 1358.32
Baseline: 4.75
Peak: 14.48
Peak 5 (Area: 335.70)
Width: 176 pts
Sum: 335.57
Baseline: 4.45
Peak: 8.40
Peak 6 (Area: 3518.50)
Width: 454 pts
Sum: 3518.26
Baseline: 5.12
Peak: 27.64
Peak 7 (Area: 1280.70)
Width: 396 pts
Sum: 1280.55
Baseline: 5.07
Peak: 15.80
Peak 8 (Area: 2427.04)
Width: 456 pts
Sum: 2426.95
Baseline: 5.15
Peak: 23.08
Amplitude
Duration (s)
+3.529e1
+5.408e1
+5.678e1
+6.501e1
+1.3747e2
+1.5898e2
+1.9075e2

事件率与Geant4模拟差距百分之几，说明阈值在O(keV)

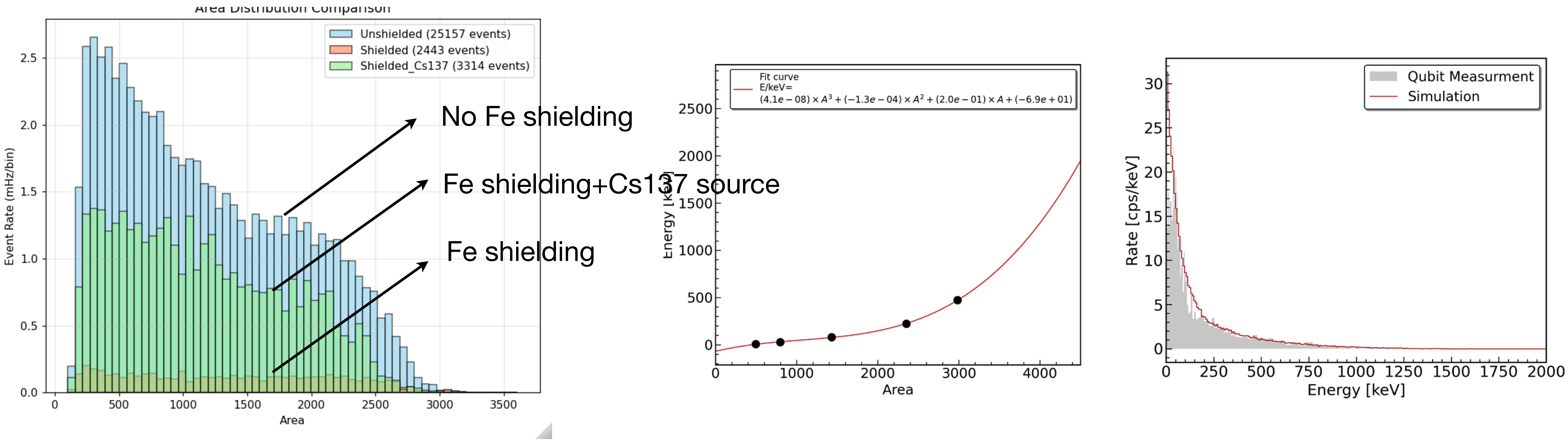

- 面积约大于3000的事件率在屏蔽前后没有明显变化，且事件率与蓝宝石内部的放射性同位素发生alpha衰变相近
- 面积约大于2600的事件率在加入Cs-137前后没有明显变化，说明放射源最大沉积能量~600 keV对应这一位置

Experimental Status

- No significant change on Area>3000 w/wo shielding, rate consistent with expectation from alpha decay in sapphire
- Event rate spectrum consistent with gamma simulations using Geant4
- Calibrated the energy deposition, spin-flip measurement sensitive to keV-MeV energy deposition
- An order of magnitude background reduction with 10 cm Fe shielding
- Low energy calibration and first data expected in 2026

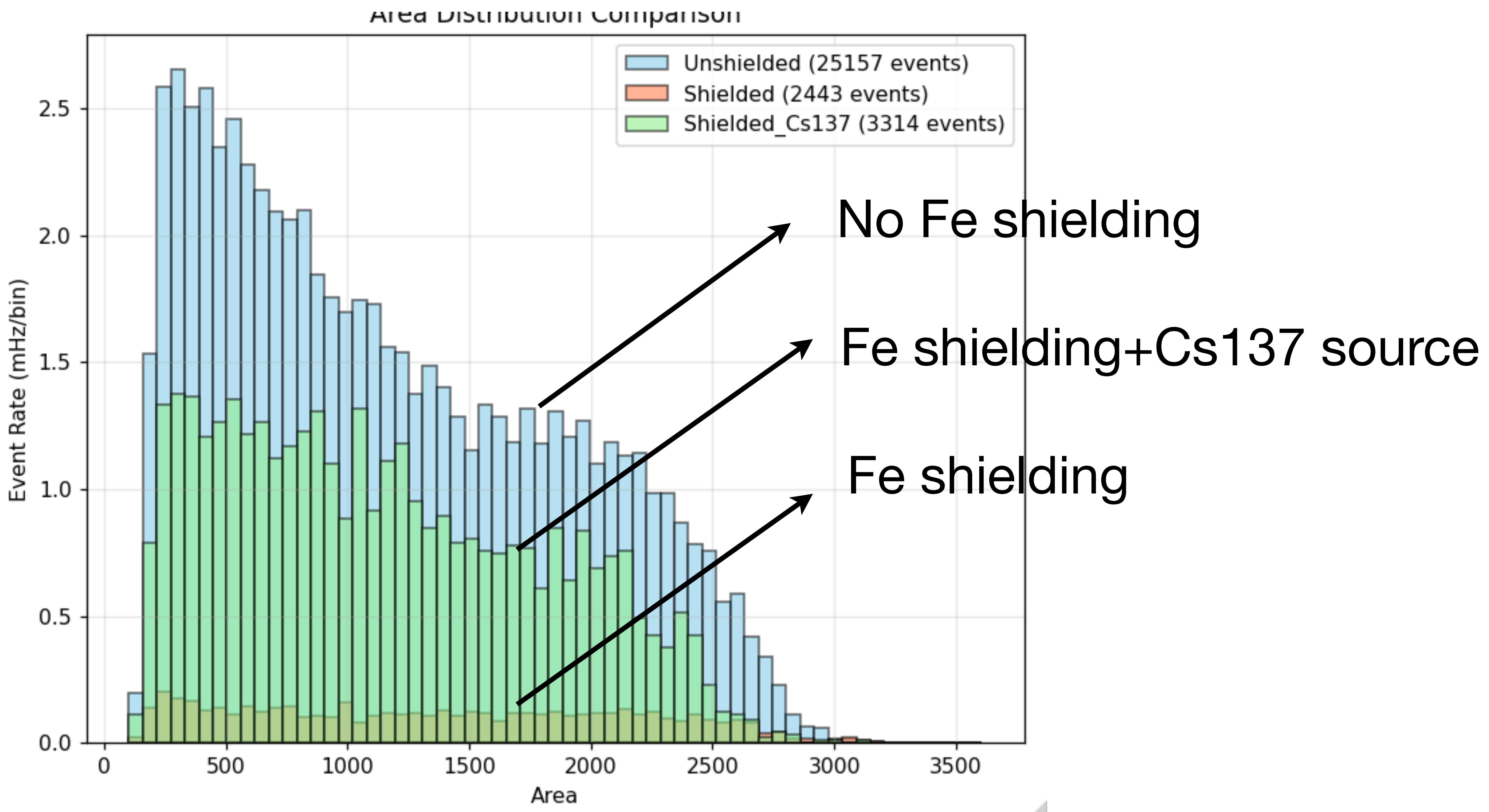

Area/energy